REDUCING THE UNCERTAINTY IN GROUNDWATER AVAILABILITY AND ITS SENSITIVITY TO LAND-USE AND CLIMATE VARIABILITY

Project Number: 2334

Public Final Report
Submitted on: December 18, 2020

Prepared for
Alberta Innovates, Mark Donner

Prepared by
University of Calgary
Masaki Hayashi, Professor, Department of Geoscience
403-220-2794, hayashi@ucalgary.ca

Alberta Innovates (AI) and Her Majesty the Queen in right of Alberta make no warranty, express or implied, nor assume any legal liability or responsibility for the accuracy, completeness, or usefulness of any information contained in this publication, nor that use thereof infringe on privately owned rights. The views and opinions of the author expressed herein do not necessarily reflect those of AI or Her Majesty the Queen in right of Alberta. The directors, officers, employees, agents and consultants of AI and the Government of Alberta are exempted, excluded and absolved from all liability for damage or injury, howsoever caused, to any person in connection with or arising out of the use by that person for any purpose of this publication or its contents.

TABLE OF CONTENTS

EXECUTIVE SUMMARY

Groundwater resources are gaining importance in Alberta, particularly in regions with increasing population and industrial activities. We need to recognize the limited availability of groundwater and manage this vital resource within the capacity of individual watersheds. As groundwater is extracted, its availability depends on the volume of storage reservoirs (i.e. aquifers) and the rate of replenishment of those aquifers. The latter is called groundwater recharge. The overall goal of this project is to advance our understanding of groundwater recharge in the unique environment of the Canadian prairies and develop practical tools for estimating recharge at various temporal and spatial scales.

Field experiments and monitoring was conducted at instrumented study sites designed to examine the effects of land-use practices and irrigation on groundwater recharge processes. The field observation demonstrated clearly that groundwater recharge is focussed under topographic depressions, where snowmelt water converges to form seasonal ponds and infiltrate rapidly during the spring thaw. This mode of recharge, called depression-focussed recharge, is the dominant mode of recharge in agricultural regions of central and southern Alberta including irrigated fields.

Guided by field observations, a simple numerical model was developed to simulate depression-focussed recharge processes. The new model is based on a widely used soil water model called Versatile Soil Moisture Budget (VSMB), which was adapted to represent recharge processes in a system consisting of a depression and surrounding uplands. Therefore, the new model is called VSMB depression-upland system (VSMB-DUS). The model simulation results were consistent with field observations at a scale of individual depressions (10^2-10^3 m^2) and at a scale of a small watershed (10^2 km^2).

VSMB-DUS was used to estimate the spatial distribution of groundwater recharge in the agricultural region (i.e. White Zone) of central and southern Alberta under the present climate and a future climate scenario representing years 2094-2100 under the 'business as usual' greenhouse gas emission. The estimated recharge amounts varied between 5 and 60 mm y^{-1} under the present climate. Under the future climate, groundwater recharge rates are expected to remain the same or slightly decline due to the reduction in snowmelt runoff. However, the climate model indicates increased amounts and intensity of rainfall during the growing season, generating high summer runoff in wet years. As a result, the timing of recharge may shift from spring to summer and the amounts may increase in wet years.

The primary benefit of this project is the spatially distributed information on groundwater recharge in the agricultural region of Alberta, and the simple numerical tool to estimate groundwater recharge at a local site using basic soil and meteorological information. This type of information is valuable for assessing the potential impacts of increased groundwater extraction at scales ranging from individual farmlands to watersheds. The secondary benefit of the project is the strengthened collaboration between the university researchers and Alberta Government departments, and the training of students and field technicians who have obtained meaningful employments using the skills learned through the project.

1. INTRODUCTION

Groundwater resources are gaining importance in Alberta, particularly in regions with increasing population and industrial activities. We need to recognize the limited availability of groundwater and manage this vital resource within the capacity of individual watersheds. Compared to surface water, however, much less is known about the available quantity of groundwater resources in Alberta, leading to a large degree of uncertainty in water security and management under the present condition. The uncertainty becomes greater considering changes in amounts and patterns of precipitation under projected future climate and the effects of changes in land use. This represents a major knowledge gap in groundwater management, which is addressed by the project. Groundwater is a renewable resource, and its availability is determined by the rate of replenishment, called recharge, not by the existing volume of groundwater. Therefore, it is critically important to understand and quantify groundwater recharge processes for sustainable management of the renewable resource. The overall goal of the project is to reduce the uncertainty in groundwater recharge estimates and provide the scientific foundation for sustainable groundwater management.

2. PROJECT DESCRIPTION

To achieve the overall goal stated above, we conducted detailed field studies of hydrological processes, and developed and refined a numerical model to simulate groundwater recharge processes. The physiography of the Canadian prairies is characterized by cold semi-arid climate and glaciated terrain. Previous studies have shown that groundwater recharge in the Canadian prairies is strongly focussed under topographic depressions, which collect snowmelt runoff and allow infiltration to exceed evapotranspiration demand. To represent these unique characteristics, a new groundwater recharge model was developed in this project. The model is based on a soil water balance model called Versatile Soil Moisture Budget (VSMB), which has been used in the Canadian prairies for agricultural water management for several decades. The new model incorporates the transfer of snow-derived water from uplands to depressions, and is called VSMB Depression-Upland System (VSMB-DUS). The specific objectives of the project are the following.

1. Determine how the mode and amount of recharge varies within the Edmonton-Calgary corridor (ECC) and the Calgary-Lethbridge corridor (CLC) region, and test the applicability of VSMB-DUS in the region.
2. Determine how recharge processes are influenced by agricultural land uses (i.e. perennial grass for cattle grazing vs. cropland under annual crop rotation) and incorporate experimental findings into VSMB-DUS.
3. Quantify how irrigation water is partitioned into evapotranspiration and groundwater recharge.
4. Examine the reliability of recharge estimates by VSMB-DUS against observed recharge fluxes at watershed scale.
5. Evaluate the sensitivity of groundwater recharge to changes in regional climate and land use.

These objectives were achieved through multiple project tasks. The performance of the project is measured with respect to the tasks as described in Section 4.6.

3. METHODOLOGY

3.1 Study sites

Field studies were conducted at several locations within the ECC and CLC region (Fig. 3.1). The region is generally covered by glacial deposits mainly consisting of glacial till, which is underlain by sedimentary rock formations from the Cretaceous to Paleogene periods (Barker et al. 2011). Groundwater in the ECC-CLC region is extracted from relatively permeable units (e.g., fractured sandstone) in bedrock formations and from surficial aquifers embedded within glacial till or deposited in buried valleys.

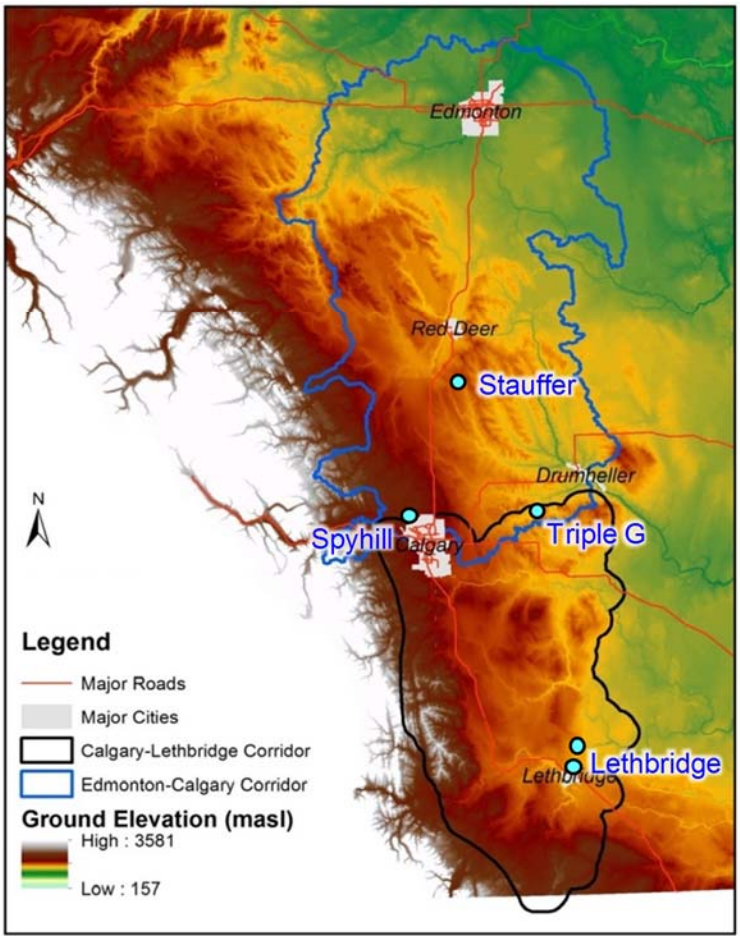

Figure 3.1 Elevation map of central and southern Alberta showing the location of instrumented study sites.

Climatic factors vary considerably within the ECC-CLC region with mean annual air temperature generally increasing and precipitation decreasing from northwest to southeast. This climatic gradient is reflected in the type of dominant vegetation, resulting in varying ecoregions from parkland to grassland. Table 3.1 lists the long-term (1981-2010) average values of air temperature and precipitation at the weather stations corresponding to the key study sites: Olds (27 km southwest of Stauffer), Calgary (17 km east of Spyhill), Gleichen (34 km south

of Triple G), and Lethbridge (7 km southwest of Lethbridge Demo Farm). The adjusted and homogenized data set (Mekis and Vincent, 2011; Vincent et al., 2012) are used to calculate the values listed in Table 3.1. The data collected at the Stauffer site were not directly used in this report, but they were used in the previous phase of the study to guide the development of process-based understanding of groundwater recharge in the ECC region.

Table 3.1 Long-term (1981-2010) mean values of air temperature and precipitation computed from the adjusted and homogenized data set, and the ecoregion of the key locations.

Long-term station	Study site	January temp. (°C)	July temp. (°C)	Annual precip. (mm)	Ecoregion
Olds	Stauffer	−8.4	15.0	514	Parkland
Calgary	Spyhill	−6.7	16.6	482	Parkland
Gleichen	Triple G	−9.8	17.1	355	Grassland
Lethbridge	Lethbridge DF	–5.6	18.8	419	Grassland

The Spyhill research site was established in 2003 as part of the larger West Nose Creek (WNC) hydrological observatory (Hayashi and Farrow, 2014). In addition to Spyhill site, the WNC observatory has a second instrumented site at Woolliams Farm (11 km northeast of Spyhill), a long-term stream gauging station, and a network of 11 groundwater monitoring wells in bedrock aquifers, established using a citizen science approach (Little et al., 2016). Hydrological monitoring systems at the Spyhill site are distributed over two contrasting land covers of annually harvested alfalfa crop and grass pasture. The pasture was grazed by cattle until 2006, but has not been grazed since then. Therefore, it is considered ungrazed grassland for the purpose of this study. The area has an undulating topography with numerous depressions, typical of the Canadian prairies. Overburden sediment in the area consists of *ca*. 10 m thick clay-rich till underlain by *ca*. 30 m thick gravel deposited on top of shale and sandstone of the Paleogene Paskapoo Formation (van Dijk, 2005). The ungrazed grassland site has a weather station equipped with sensors for air temperature, humidity, wind speed, radiation, precipitation; an eddy-covariance system for measuring evapotranspiration; soil moisture and temperature sensors; and a large number of groundwater monitoring wells with depths ranging between <1 m and 40 m (see Hayashi et al., 2010 and Mohammed et al., 2013 for details).

The Triple G location has two separate sites, 1.7 km apart, consisting of grazed grassland (established in November 2014) and annual cropland (established in June 2017). The area has an undulating topography covered by at least 15 m of clay-rich glacial till underlain by the Scollard Formation bedrock (Fig. 3.2).

The Triple G grassland site had been seeded with meadow brome grass (*Bromus riparius*) and used for cattle grazing from May to August at an estimated intensity of 0.4 animal per hectare; however, it was not grazed during the 2017 growing season. The cropland site was under a four-year crop rotation with direct seeding (i.e. zero tillage), and had been under zero-tillage management for two decades, representing a typical condition of the region. It was planted with spring wheat (*Triticum aestivum*) in 2017 and 2018, and yellow mustard (*Sinapis alba*) in 2019. The stubble in the cropland was grazed by cattle after harvest at a similar intensity as the grassland, typically from September to December.

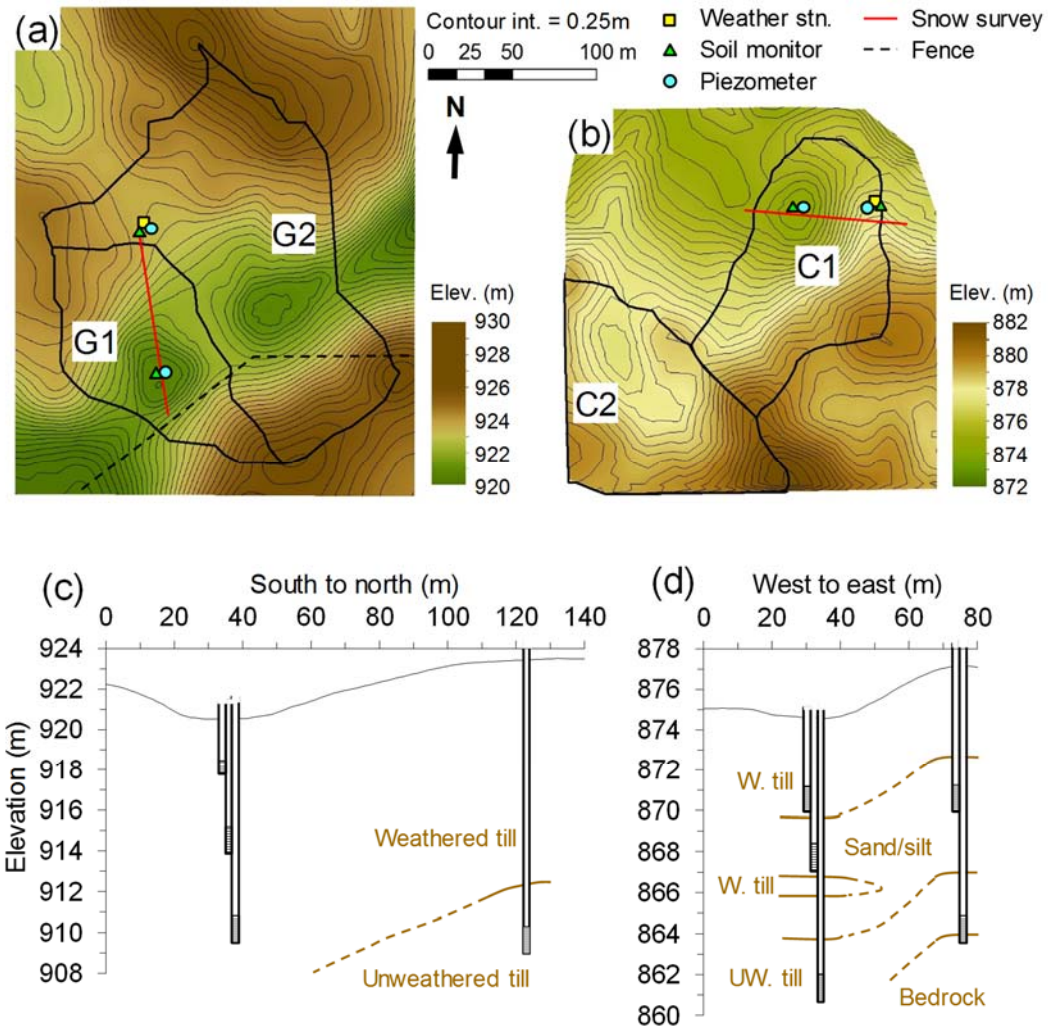

Figure 3.2 Location of field monitoring sites at the Triple G grassland (a) and cropland (b), and hydrogeological cross sections showing piezometer depths at the grassland (c) and the cropland (d). Glacial tills are differentiated into weathered (W) and unweathered (UW).

The Lethbridge Demo Farm (LDF) was the primary site for the irrigation study and was located less than 2 km east of the Lethbridge city limits (Fig. 3.3a). LDF consisted of ten fields, eight of which were irrigated with central pivot, variable-rate irrigation systems and two of which were under dryland cultivation (Fig. 3.3c). A secondary site was chosen at the Perry Produce (PP) property, located approximately 25 km northeast of Lethbridge (Fig. 3.3a), for borehole drilling and sampling. The PP site consisted of one 80-hectare central irrigation pivot system and four dryland corners (approximately 15 ha each) (Fig. 3.3b). Typical crops in the region include wheat, barley, canola and specialty crops such as corn, potatoes, sugar beets, alfalfa and peas (Rodvang, 2002).

Both Lethbridge area sites are located within the St. Mary River Irrigation District, which receives water from the St. Mary River, Waterton River, and Belly River, ultimately fed from headwaters originating in the Rocky Mountains to the west. The region surrounding the LDF and PP sites is characterized by flat to gently undulating glacial sediments to depths of up to 80

meters (Rodvang, 2002; Shetsen, 1987; MacCormack et al., 2015). According to a previous study, the LDF site is directly underlain by about 2 m of glaciolacustrine sediments that overlie clay till deposits (Rodvang, 2002), resulting in relatively flat local topography. The geology surrounding the PP site is generally similar, but surficial deposits consist of predominantly moraine till, with isolated lenses of gravel, sand and silt (Shetsen, 2005). This produces a more undulating terrain with average local relief ranging from 3-10 m (MacMillan and Pettapiece, 2000; Shetsen, 1987).

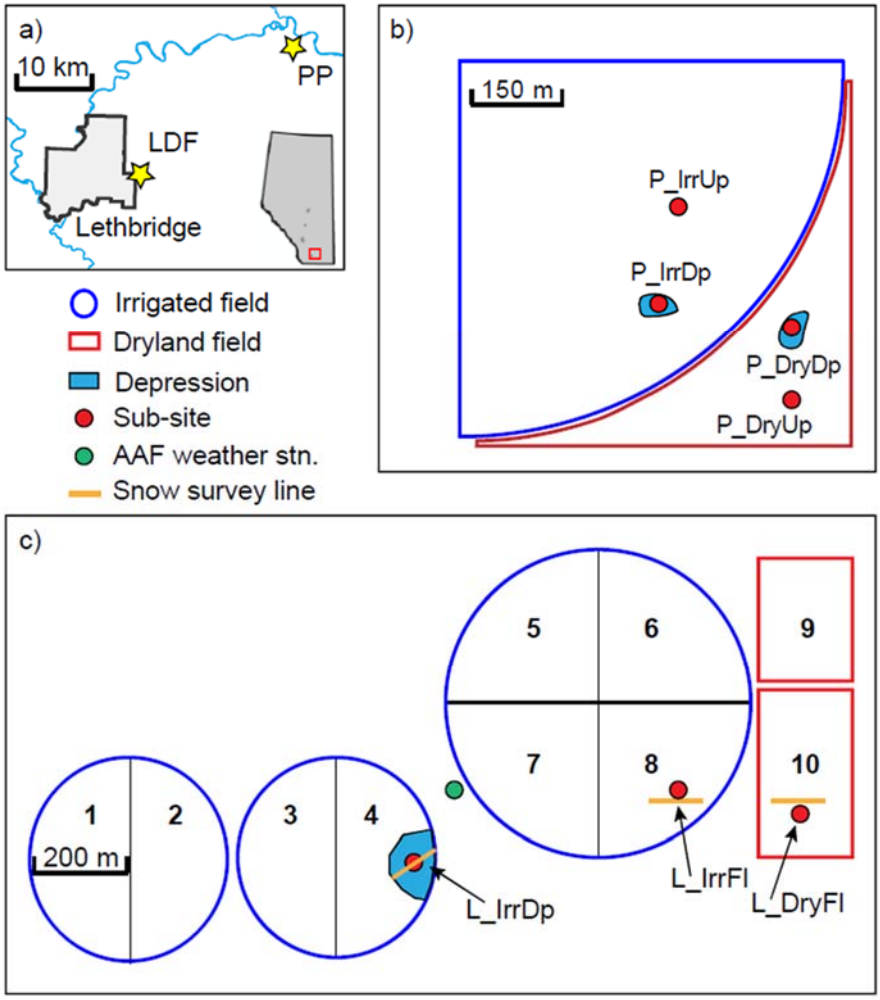

Figure 3.3 (a) Location and layout of Lethbridge area study sites. (b) Perry Produce (PP) site consisted of four sub-sites. (c) Lethbridge Demonstration Farm (LDF) consisted of three sub-sites. AAF = Alberta Agriculture and Forestry station.

3.2 Field and laboratory methods

3.2.1 Field instrumentation and measurement at the Triple G site

Nearly identical sets of instruments and methods were used at the Triple G grassland and cropland sites to compare the key hydrological processes under the two most common

agricultural land uses in central and southern Alberta. Two depressions at each site were used to estimate snowmelt runoff in the respective catchments (Fig. 3.2), and G1 (grassland) and C1 (cropland) were instrumented for monitoring groundwater levels, soil moisture, and soil temperature. The areas of the depressions and their catchments are listed in Table 3.2. Each site had a meteorological station on the upland adjacent to the instrumented depression (Figs. 3.2a and 3.2b), equipped with an air temperature and humidity sensor, a radiometer, an eddy-covariance system for monitoring evapotranspiration, and a ground heat flux plate. Precipitation was measured by Alberta Agriculture and Forestry at the Standard meteorological station located 4 km north of the cropland site. Soil moisture and temperature sensors were installed at upland and depression locations at several depths from 0.2 to 1.5 m, and piezometers were installed with screen depths ranging from 3 to 15 m (Figs. 3.2c and 3.2d). Details of site instrumentation are described by Morgan (2019).

Snow water equivalent (SWE) was determined by conducting snow surveys after major snowfall events along 100-m transects encompassing the upland and the depression (Figs. 3.2a and 3.2b). Snowmelt runoff was estimated from the volume of water collected in depressions during runoff events. Note that all depressions were dry prior to snow accumulation, and ponds formed as a result of snowmelt runoff. At each depression shown in Fig. 3.2, a detailed elevation survey was conducted to determine the catchment area and the values of coefficients in pond depth-area-volume functions (Hayashi and van der Kamp, 2000).

Sediment samples were collected from the boreholes during piezometer installation at 0.3–0.8 m intervals, and groundwater samples were collected from the piezometers (see Morgan, 2019 for details). Pond water samples were collected from G1 and C1 at regular intervals (every 1–2 weeks) while the depressions were ponded. Pore-water anions in sediment samples were extracted following the procedure described by Parsons et al. (2004). All water samples were analysed for major anions using an ion chromatograph. Groundwater samples were analyzed for tritium concentration using the liquid scintillation counting method preceded by sample enrichment by electrolysis with a nominal detection limit of 0.8 tritium unit (TU) at University of Waterloo Environmental Isotope Laboratory.

Table 3.2 Catchment area (A_c), depression area (A_d), and scale (s) and shape (p) parameters of the four depressions at the Triple G Farm. Depression area is defined by the highest water level recorded during 2017–2019 using the depth-area-volume relation.

Depression		A_c (m^2)	A_d (m^2)	s (m^2)	p (-)
Grassland	G1	9793	1247	1752	1.80
	G2	22129	1948	2888	1.73
Cropland	C1	10620	1076	2070	2.07
	C2	11417	1311	3413	1.78

3.2.2 Field instrumentation and measurement at Lethbridge sites

Three sub-sites were instrumented at LDF: an irrigated depression in Field 4 (denoted L_IrrDp), irrigated flatland in Field 8 (L_IrrFl) and dryland flatland in Field 10 (L_DryFl) (Fig. 3.3c). In this report, "L_" and "P_" designate the LDF and PP study sites, respectively. "Irr" and "Dry" designate irrigated and dryland conditions and "Fl", "Up", "Dp" designate flatlands, uplands and depressions, respectively. In order to observe spatial and temporal differences in hydraulic response to precipitation and irrigation events, as well as differences in surface radiation fluxes, several levels of instrumentation were used. Each of the three instrumented sub-sites included a tipping bucket rain gauge to measure precipitation and irrigation, while the irrigated (L_IrrFl) and dryland (L_DryFl) fields were equipped with meteorological stations. Eddy-covariance systems for measuring evapotranspiration were deployed in the irrigated field (L_IrrFl) in 2017 and in the dryland field (L_DryFl) in 2018. A vertical array of soil moisture and temperature probes were deployed to a depth of 1.5 m at each of the three instrumented locations in 2017, with vertically nested tensiometers added in 2018. All fields were planted with barley for the 2017 growing season. In the following year (2018) L_IrrDp was planted with barley, L_IrrFl with sugar beets, and L_DryFl with canola.

In addition to the above instrumentation, boreholes were drilled at both the LDF and PP sites in 2017 to collect sediment samples and piezometers were installed at the LDF site. Eight boreholes were drilled at the LDF site, with continuous coring and sediment samples collected in the three deepest boreholes (one at each sub-site). Piezometer nests were installed at each LDF sub-site to record groundwater levels and vertical gradients, and to collect water samples. Four additional boreholes were drilled and sampled at the secondary PP site: an irrigated upland (P_IrrUp), irrigated depression (P_IrrDp), dryland upland (P_DryUp) and dryland depression (P_DryDp) (Fig. 3.3b). Porewater extracts from all sediment samples were analyzed for chloride and stable isotopes (^{2}H and ^{18}O) and were compared to precipitation, irrigation, groundwater and surface water samples in order to identify the source and rate of groundwater recharge. Weekly snow surveys were conducted at the LDF site in the winter of 2017-2018 along 100-m long transects at each sub-site (Fig. 3.3c).

3.2.3 Chloride mass balance method for recharge estimation

Chloride mass balance (CMB) is commonly used to estimate long-term average groundwater recharge in semiarid regions (e.g., Scanlon et al., 2006). We have modified the conventional CMB method for its application to depression-focussed recharge, accounting for the lateral transfer of chloride by snowmelt runoff (Pavlovskii et al., 2019). Recharge rates under the current land uses were estimated using:

$$R_d = (PC_p + Q_{in} + Q_{lat} A_u/A_d) / C_d \quad (1)$$

where R_d (m y^{-1}) is the recharge rate under the depression, P (m y^{-1}) is annual precipitation, C_p is the chloride concentration in precipitation (g m^{-3}), Q_{in} (g m^{-2} y^{-1}) is the chloride deposition rate in the depression due to anthropogenic sources such as fertilizer, Q_{lat} (g m^{-2} y^{-1}) is the lateral chloride transport rate from the uplands to the depression, A_u (m^2) is the upland area, A_d (m^2) is the depression area, and C_d (g m^{-3}) is the pore-water chloride concentration under the depression. When the mass balance over a long time period (e.g., > 10^3 years) prior to agricultural activity (i.e. Q_{in} = 0) is considered, the chloride cycle within a depression-upland catchment reaches a quasi-steady state (Hayashi et al., 1998), and a simpler form of equation

can be used to estimate catchment-scale recharge (R_{cat}):

$$R_{cat} = PC_p / C_{gw} \quad (2)$$

where C_{gw} (g m^{-3}) is the average groundwater chloride concentration in the catchment (Pavlovskii et al., 2019).

3.3 VSMB-DUS model

The Versatile Soil Moisture Budget (VSMB) model is widely used to simulate soil water balance in the Canadian prairies for agricultural applications (e.g., Government of Alberta, 2019). Since the development of the original VSMB by Baier and Robertson (1966), it has undergone a series of improvements by Akinremi et al. (1996), Hayashi et al. (2010), and Mohammed et al. (2013) to represent relevant hydrological processes in a more physically-based manner including an improved representation of snow and frozen soil processes and macropore infiltration in frozen soil.

The VSMB in this study calculates soil water balance on a daily basis for seven soil layers (five for depression) with thicknesses ranging between 0.1 m and 2.0 m (Fig. 3.4). The calculation starts with the addition of precipitation to the soil column depending on the season. The Utah Energy Balance model (Tarboton and Luce, 1996) is used with winter precipitation data to simulate snowpack evolution and calculate snowmelt input, whereas summer precipitation is applied directly to the soil surface after interception loss is subtracted. When the top soil layer is unfrozen, runoff is estimated using the Curve Number method (Natural Resources Conservation Service, 2004). When the top soil layer is frozen and unsaturated, snowmelt water cannot infiltrate into the next layer until the top layer reaches saturation. The liquid water infiltrates into the next layer if the added water exceeds the saturation limit; the infiltration rate in this process is limited by a user-specified constant (f_{lxm}, m s^{-1}) representing the effects of soil macropores (Mohammed et al., 2013). The remaining excess water is routed to generate runoff. After the infiltration into the top soil layer, water is subsequently distributed to lower layers by gravity drainage and gradient-driven moisture diffusion. The evapotranspiration rate from each soil layer is individually calculated based on soil moisture, meteorological forcings, and plant growth stage.

Depression-focussed groundwater recharge is estimated using VSMB Depression-Upland System (VSMB-DUS), which couples vertical soil water balances of the depression and the upland via lateral runoff from the upland to the depression (Noorduijn et al., 2018) (Fig. 3.4). In VSMB-DUS, runoff from the upland accumulates the depression and form a pond when the volume of water inputs to the depression exceeds the infiltration capacity of the soil column. The pond area can reach its maximum (A_{pmax}) when pond water rises to the spill point, and as a result, the excess water generates overflow (O) leaving the depression. Losses from the ponded water can occur through direct evaporation from the water surface at the potential evaporation rate. Other losses can occur by infiltration to the underlying soil layer, including lateral subsurface flow to the unflooded area within the depression. The underlying soil layers may reach saturation under sustained infiltration. The amount of groundwater recharge is given by the drainage flux from the deepest soil layer. The bottom drainage flux is restricted by a model parameter (f_{bmax}, m s^{-1}) representing the combined effects of the hydraulic gradient and the hydraulic conductivity of clay-rich glacial till underlying the soil column. The drainage fluxes

from the bottom of the two soil columns (R_u and R_d, Fig. 3.4) are weighted according to the relative areas of upland and depression to estimate catchment-average groundwater recharge.

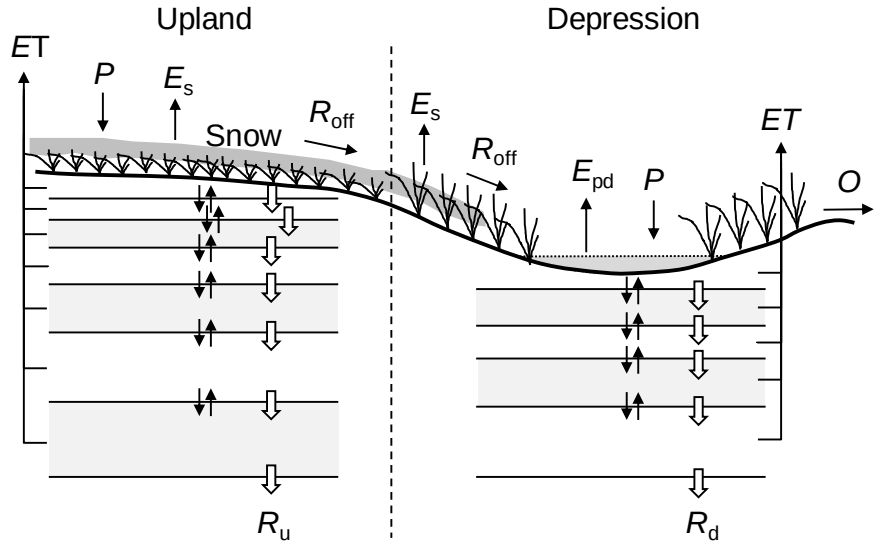

Figure 3.4 Conceptual framework of VSMB-DUS consisting of upland and depression showing precipitation (P), vapour flux from snowpack (E_s), soil evapotranspiration (ET), runoff (R_{off}), pond evaporation (E_{pd}), and the possibility of depression overflow (O). Open arrows indicate gravitational drainage and thin solid arrows indicate moisture diffusion. The drainage at the bottom of the soil profiles gives recharge from upland (R_u) and depression (R_d). Modified after Noorduijn et al. (2018).

3.4 Upscaling methodology

3.4.1 Application of VSMB-DUS to regional-scale recharge estimation

VSMB-DUS estimates groundwater recharge for an individual depression-upland system. For regional-scale groundwater management, it would be necessary to run VSMB-DUS for a large number (10^4–10^5) of depressions, which is not a practical approach. A statistical upscaling approach provides a more efficient alternative for regional-scale estimates while capturing important local characteristics of topography, climate, and land use.

Detailed methods for obtaining topographic parameters are described by Pavlovskii et al. (2020). Briefly, high-resolution (2 m) digital elevation model (DEM) of a representative area (6500 km^2) was used to extract all topographic depressions in the area and determine the areas of individual depressions (A_d) and their catchments (A_c), as well as the coefficients in the equations describing the area-volume relationship of depression ponds. The surficial geology of the agricultural regions of central and southern Alberta is dominated by four types of glacial landforms, namely moraine, stagnant ice moraine, fluted moraine, and glaciolacustrine deposits (Fenton et al., 2013) (Fig. 3.5). For each of the four dominant landforms, the probability distribution of A_d and A_c were determined, along with the mean values of coefficients representing the area-volume relationship of all depressions within each landform type.

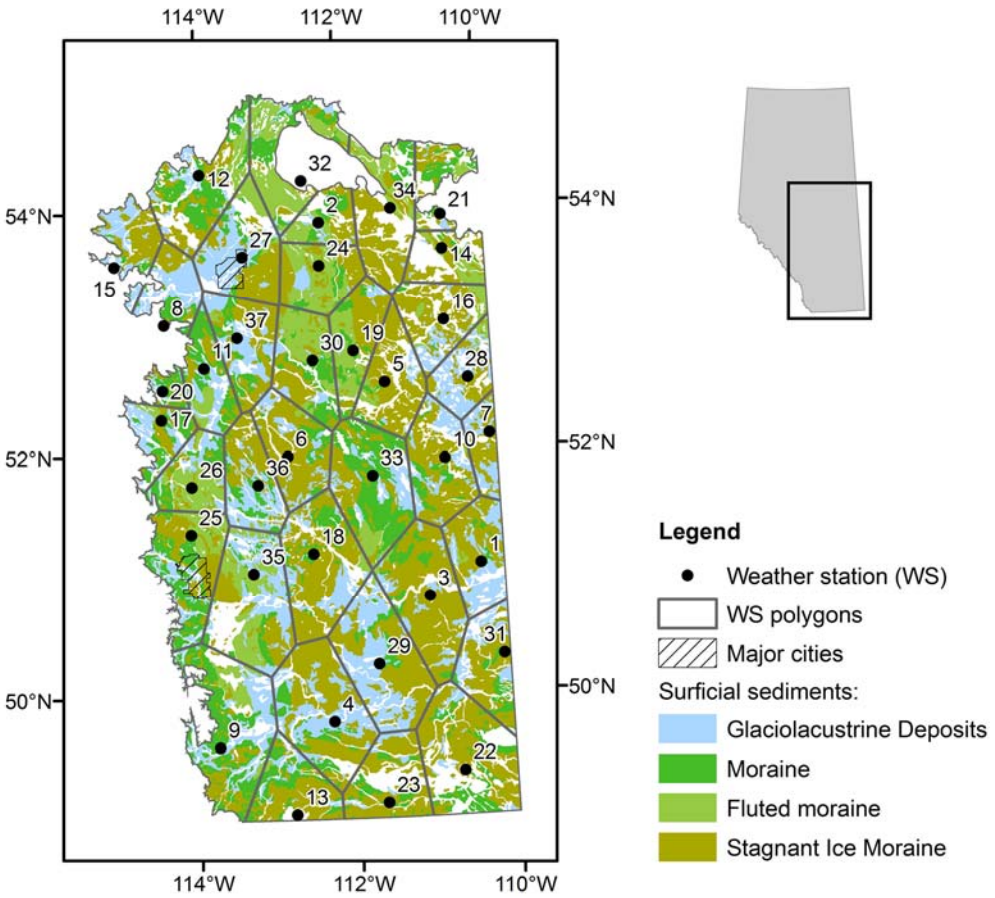

Figure 3.5 Distribution of surficial sediment/landform types (Fenton et al., 2013) and Thiessen polygons for the 37 weather stations. The blank areas are covered by the sediments other than the four major types. The names of the weather stations are listed in Table 3.3.

The agricultural region was divided up into 37 polygons represented by weather stations providing the meteorological forcing data for VSMB-DUS (Fig. 3.5, Table 3.3). Hourly meteorological data for the simulation period of November 2009 – October 2016 were obtained from Alberta Agriculture and Forestry. For each of the 37 polygons, VSMB-DUS was run for 196 combinations of topographic variables and the mean recharge was calculated using the probability distribution of these variables. These were based on 14 values of A_c ranging from 100 to 819,200 m^2 and 14 values of A_d/A_c ranging from 0.01 to 0.95. The procedure was repeated twice to calculate recharge values for two dominant land uses in the region, namely grazed grassland and cropland.

Table 3.3 List of the weather stations providing the meteorological data used in VSMB-DUS simulations for the agricultural region of Alberta.

ID	Name	ID	Name	ID	Name	ID	Name
1	Acadia Valley	11	Dapp	21	Manyberries	31	Smoky Lake
2	Andrew	12	Del Bonita	22	Masinasin	32	Spondin
3	Atlee	13	Dewberry	23	Mundare	33	St. Paul
4	Barnwell	14	Evansburg	24	Neir	34	Strathmore
5	Bellshill	15	Gilt Edge North	25	Olds College	35	Three Hills
6	Big Valley	16	Hespero	26	Oliver	36	Wetaskiwin
7	Bodo	17	Hussar	27	Ribstone South	37	Smoky Lake
8	Breton Plots	18	Killam	28	Rolling Hills		
9	Brocket	19	Leedale	29	Rosalind		
10	Consort	20	Lindbergh	30	Schuler		

3.4.2 Groundwater flow model of the West Nose Creek watershed

To evaluate the efficacy of the application of VSMB-DUS to watershed-scale groundwater models, the three-dimensional groundwater flow model of the West Nose Creek (WNC) watershed developed by Niazi et al. (2017) was adapted for this study, as described in detail by Abdrakhimova (2020).

Briefly, the model was constructed using FEFLOW (Diersch, 2014) with 13 model layers to represent the hydrostratigraphy of the watershed. Two upper layers of the model represented surficial sediments, separated into several zones of hydraulic conductivity, based on the soil type. The hydraulic conductivity field of the bedrock layers 3–12 was assigned from a sand fraction map which was generated from lithological well logs (Niazi et al., 2017). The specified flux boundary at the top of the model was assigned using recharge estimates obtained from upscaled VSMB-DUS model results. The WNC watershed contained four recharge zones defined by two weather stations and two landform types.

The model was first calibrated in a steady-state mode forced by long-term average recharge using the average water level data recorded at the 11 monitoring wells (see Section 4.4). After successful calibration, the model was utilized in a transient mode using different recharge time series for the four recharge zones. The recharge time series had monthly time step, with recharge values at each step estimated by taking the average of a daily upscaled VSMB-DUS recharge rate during calendar months.

3.5 Climate model downscaling and global warming scenario

The outputs of general circulation models (GCMs) are too coarse for hydrological applications. Weather Research and Forecasting (WRF) is a numerical weather prediction

system used for atmospheric forecasting and dynamical downscaling of low-resolution climate products (Skamarock, 2008). High-resolution atmospheric models such as WRF are needed to represent fine-scale processes such as convective summer storms common in the Canadian prairies (Li et al., 2019).

Despite recent improvements in the representation of atmospheric processes in climate models, there are still large biases (i.e. mismatch) between atmospheric model outputs and observations, which need to be corrected (e.g., Teutschbein and Seibert, 2012). This study used a bivariate quantile mapping method (Cannon, 2018) to correct the model biases for air temperature and precipitation in the control period first and then the future projection. The bias-corrected WRF model outputs with 4 km horizontal grids and 37 vertical levels were used under the present climate (HY2007−2015) and under a future warming projection (HY2092–2100) to study the future changes in an upland-depression hydrological system. Note that a hydrological year (HY) in this study starts on November 1 and ends on October 31, coinciding with the start of soil freezing in most years.

The model was forced with 0.703° × 0.703° resolution, 6-hourly ERA-Interim reanalysis product, the latest global atmospheric reanalysis produced by the European Centre for Medium-Range Weather Forecasts (ECMWF) (Dee et al., 2011) for the base period, HY2007–2015. To generate the meteorological data under a warmer condition in HY2092–2100, the HY2007–2015 time series were perturbed by climatological change factors. The change factors were obtained by subtracting future projections under the representative concentration pathway of 8.5 W m^{-2} (RCP8.5) from the control period (October 2000 – September 2015). This future projection used an ensemble of more than 60 GCMs in the Coupled Model Intercomparison Project Phase 5 (CMIP5) for HY2092–2100. This approach, referred to as the pseudo global warming (PGW) method, is commonly used to dynamically downscale climate model projections (e.g., Li et al., 2019).

4. RESULTS

4.0 Organization of the results

The results are presented in the following sections organized according to the five major project tasks (see Section 4.6 for the task list).

4.1 Spatial distribution of groundwater recharge

Spatial distribution of groundwater recharge is estimated for the agricultural region of central and southern Alberta using the VSMB-DUS model. To gain confidence in model performance, VSMB-DUS was tested using the archived long-term (2006–2015) meteorological and hydrological data collected at the ungrazed grassland of the Spyhill site. The model parameters controlling evapotranspiration were adjusted to minimize the difference between model-simulated and observed evapotranspiration from the upland (Fig. 4.1). The parameters controlling snowmelt, and soil water retention and drainage were also adjusted to minimize the difference between simulated and observed snow water equivalent (Fig. 4.2b), soil temperature (Fig. 4.2c-4.2e), and soil water content (Fig. 4.2f and 4.2g). The parameter controlling

macropore infiltration in frozen soil was optimized to match the simulated and observed snowmelt runoff. The optimized model was used to estimate annual recharge amounts for HY2007–2015 (Fig. 4.3). Recharge amounts had a large interannual variability reflecting the variability in weather conditions, especially precipitation amounts.

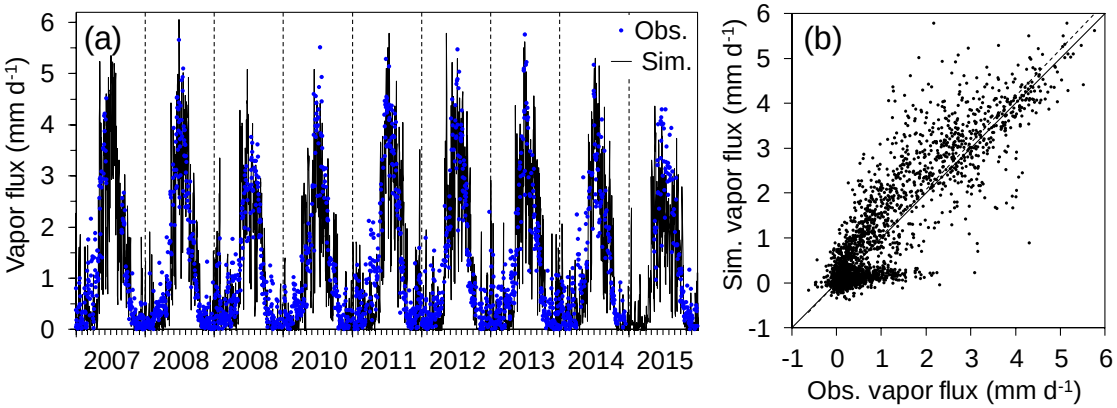

Figure 4.1 (a) Observed and simulated daily average vapor flux at the Spyhill site. Vertical lines indicate January 1 of each calendar year. (b) Observed and simulated vapor flux with the 1:1 line (solid) and the best-fit line (dashed) with a slope of 1.04.

The same model was used to estimate recharge rates in the West Nose Creek watershed. This is considered an 'upscaled' recharge estimate for grasslands. Following the upscaling methodology of Pavlovskii et al. (2020), the watershed is divided into 'stagnant ice moraine' and 'moraine' (Fig. 4.4), where the former has a higher degree of topographic relief and a larger depression storage capacity. The two subregions were further divided into polygons associated with Spyhill weather station and Woolliams Farm weather station (Fig. 4.4), whereby the meteorological data from the respective stations were used to drive the model. The average recharge rate over HY2007-2015 varied from 10 to 22 mm y^{-1} depending on the polygon (Fig. 4.5c). Area-weighted average recharge rates over the entire watershed had a high interannual variability, which was similar to the variability of the baseflow of West Nose Creek (Figs. 4.5a and 4.5b). Comparison of the simulated recharge amounts and the creek baseflow indicates that VSMB-DUS provides reasonable estimates of recharge at the scale of a small watershed (250 km^2).

To evaluate the spatial distribution of recharge at a greater scale, VSMB-DUS was applied to the entire agricultural area of central and southern Alberta encompassing the ECC-CLC region. The area was divided into a large number of subregions according to the types of surficial deposits (Fig. 3.5), and each subregion was assigned the probability distribution of depression storage as described in Section 3.4. Meteorological data recorded at 37 weather stations during HY2010-2016 were used to drive VSMB-DUS in each polygon associated with a weather station (Fig. 3.5). VSMB-DUS was run with two sets of soil and vegetation parameters representing grazed grassland and annual croplands (see Section 4.2 below), which are the two dominant agricultural land uses in the region. Estimated recharge rates mostly ranged 5–50 mm y^{-1} for grasslands and 5–60 mm y^{-1} for croplands (Fig. 4.6). The rates were generally higher in northwestern parts of the region and decreased toward the southeast, reflecting the climatic

gradient, whereby the difference between precipitation and potential evaporation (P – PET) generally decreases southeastwards.

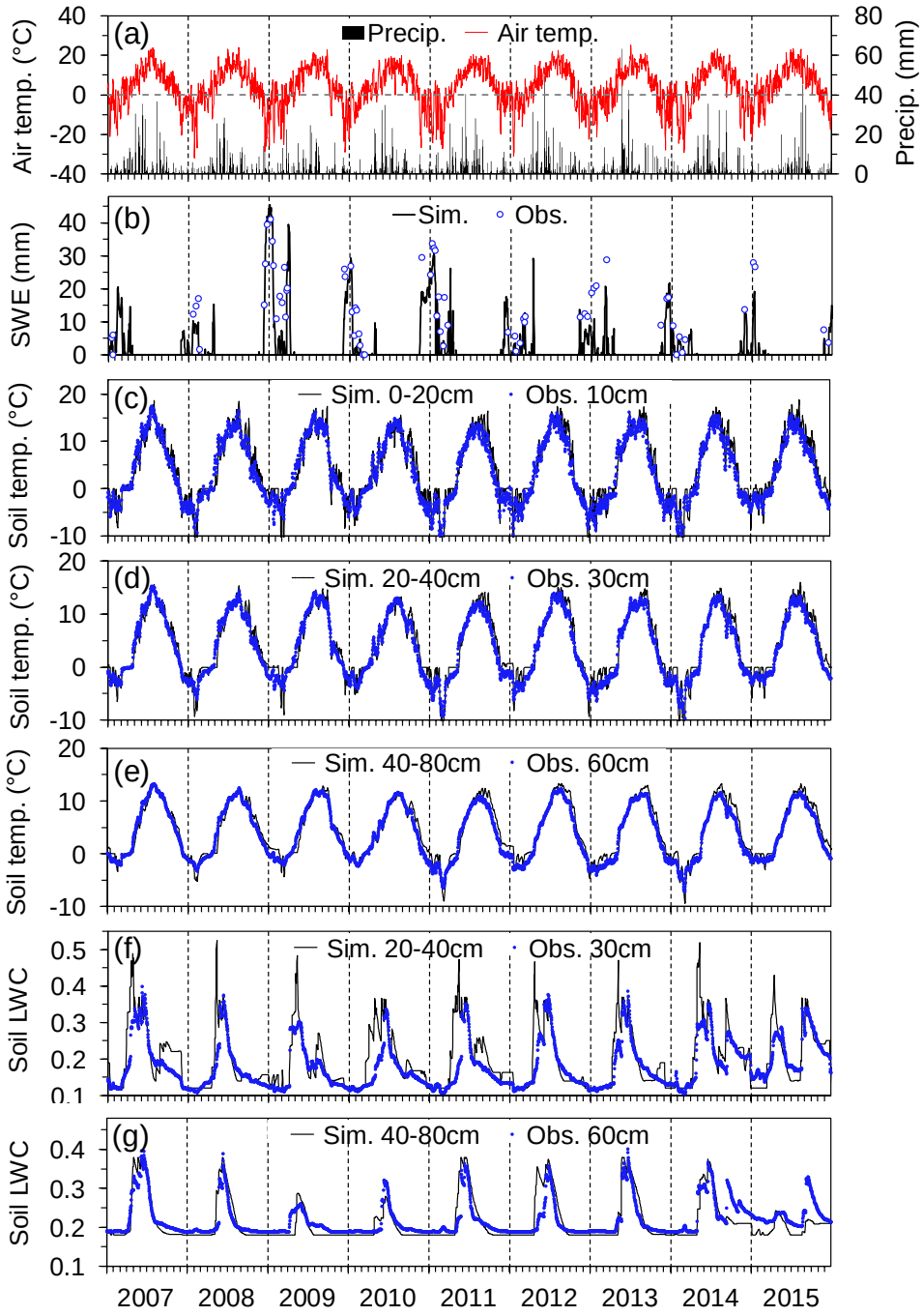

Figure 4.2 (a) Observed daily precipitation and daily mean air temperature. Vertical lines indicate January 1 of each calendar year. (b) Observed and simulated snow water equivalent (SWE). (c) Observed and simulated soil temperatures at 10 cm depth, with simulated temperature represented by the average of 0-10cm and 10-20cm model layers. (d) Soil temperatures at 30 cm depth. (e) Soil temperatures at 60 cm depth. (f) Observed and simulated soil liquid water contents (LWC) at 30 cm depth. (g) Soil LWC at 60 cm depth.

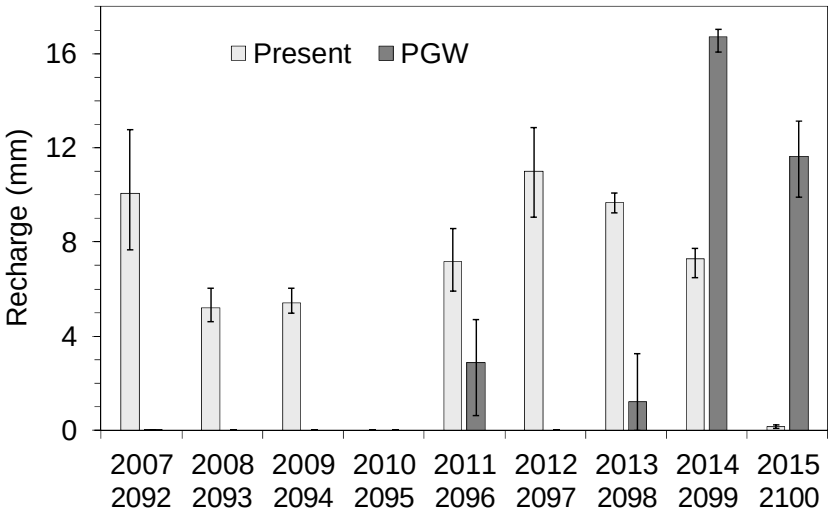

Figure 4.3 Catchment-average annual groundwater recharge simulated for the four depressions under the present climate (HY2007-2015) and the pseudo global warming (PGW) scenario for the corresponding years (HY2092-2100). Each bar indicates the average of the four depressions with a line showing the range of values.

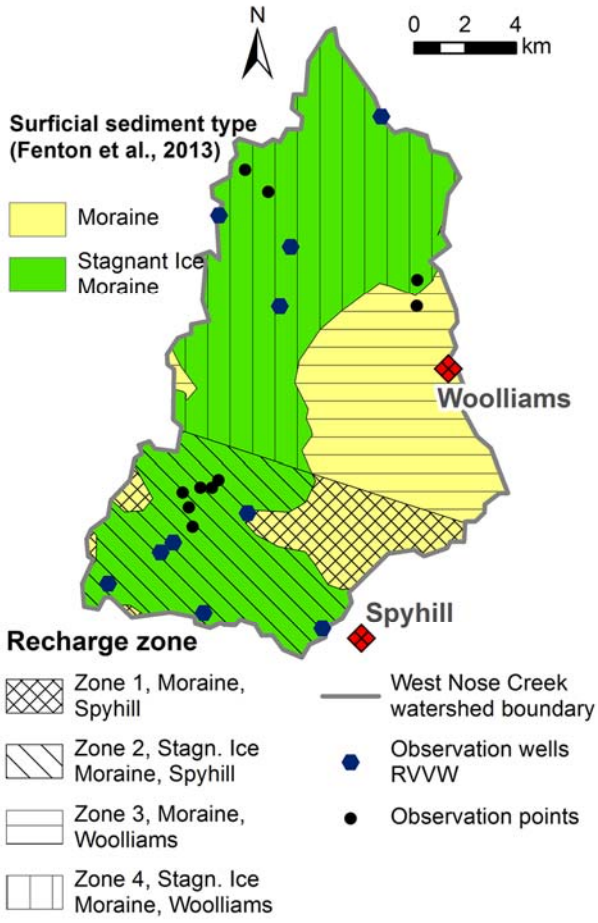

Figure 4.4 Surficial sediment/landform types (Fenton et al., 2013a) within study area. Minor polygons of other than Moraine and Stagnant Ice Moraine surficial sediment types (not shown, less than 2% of the area) are lumped to the closest polygon of Moraine or Stagnant Ice Moraine.

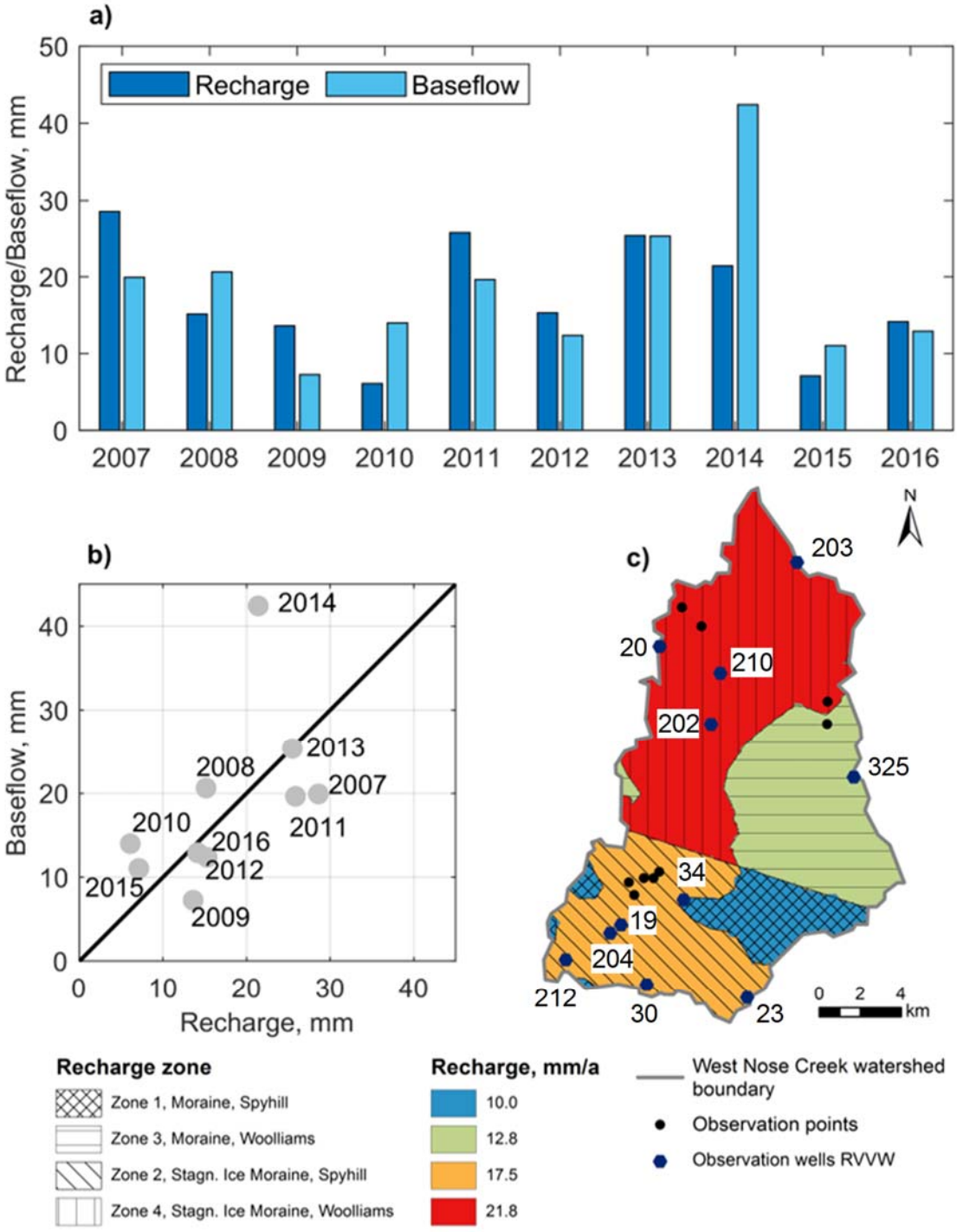

Figure 4.5 (a) Area-weighted modeled recharge for grasslands at the WNC watershed in comparison with measured baseflow. (b) Correlation between modeled recharge and measured baseflow. (c) The spatial distribution of modeled groundwater recharge and the location of observation wells selected from the Rocky View Well Watch (RVWW) network.

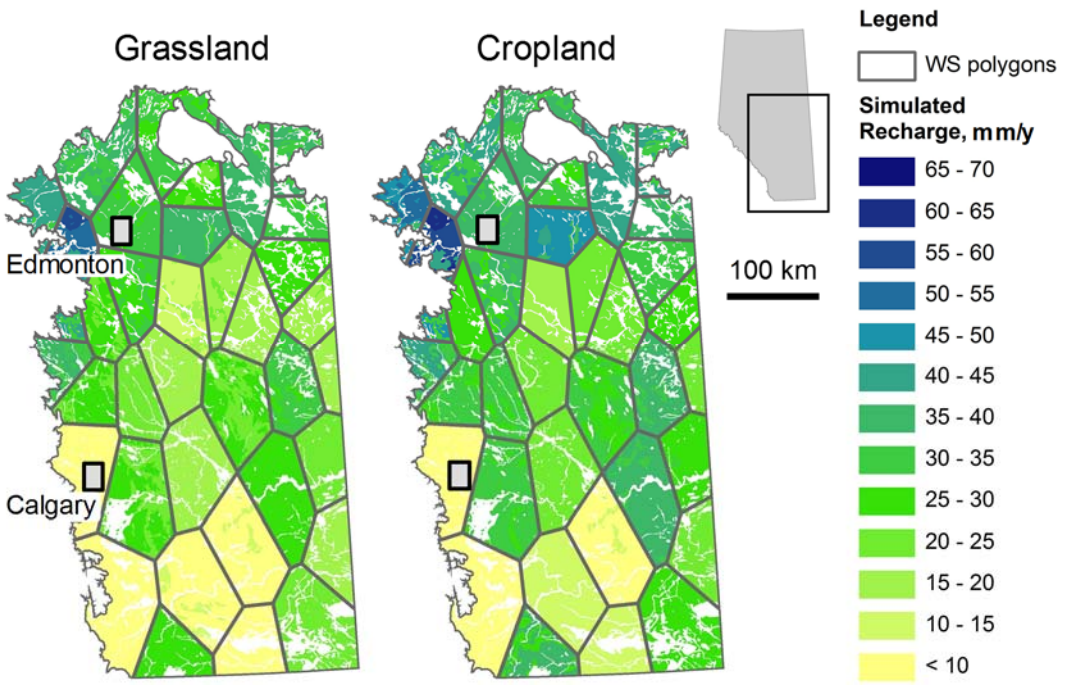

Figure 4.6 Distribution of average groundwater recharge rates during HY2010-2016 simulated by VSMB-DUS in the agricultural regions of central and southern Alberta.

4.2 Land-use comparison of groundwater recharge

Previous studies on land-use effects on the Canadian prairie hydrology were focussed on differences between annual croplands and ungrazed grasslands set aside for waterfowl habitats (e.g., van der Kamp et al., 2003). However, most grasslands in the ECC-CLC region are used for cattle grazing, and are expected to have different hydrological characteristics from ungrazed grasslands. Therefore, the focus of this study is the comparison between grazed grassland and croplands. The results of a paired-catchment study at Triple G site is summarized first, followed by a larger scale study in the West Nose Creek watershed.

Snow accumulation and snowmelt runoff have a strong influence on depression-focussed recharge, as they determine the amount of snowmelt water collected in depressions. Hereafter, pre-melt SWE refers to the snow water equivalent measured 1–2 weeks before the main snowmelt event in 2018 and 2019. Pre-melt SWE had a positive correlation with total precipitation between November 1 and the snow survey date at both grazed grassland and cropland sites (Fig. 4.7a). The grassland had a higher SWE than the cropland in both 2018 and 2019. Comparison of snow depth data indicate that the difference is attributed to large snow accumulation at the depression end of the grassland survey line (Figs. 4.7b and 4.7c), where the deposition of eastward drifting snow in the depression is enhanced by the fence line (Fig. 3.2a). The fence itself is constructed from relatively thin barbed wires, but tall vegetation growing along the fence line effectively traps drifting snow. Pre-melt SWE at the grassland site exceeded precipitation amount in 2018 (Fig. 4.7a), indicating that the fence line and the depression served as a snow sink (van der Kamp et al., 2003; Fang and Pomeroy, 2009).

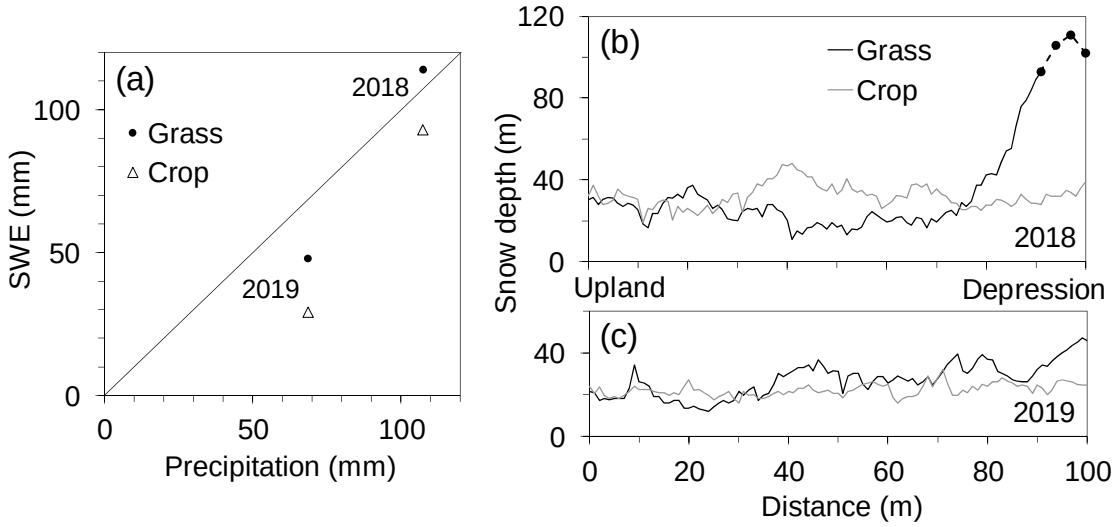

Figure 4.7 (a) Relation between winter precipitation and pre-melt snow water equivalent (SWE) at the grassland (2017−2019) and the cropland (2018−2019) of Triple G Farm. The solid line indicates a slope of 1:1. (b) Pre-melt snow depth at the grassland and the cropland on April 10, 2018. For the grassland, solid circles indicate total snowpack including a drift over an ice layer. (c) Pre-melt snow depth at the two sites on March 8, 2019. The snow survey lines start from the upland and end on the depression (see Fig. 3.2),

The main runoff event in 2018 started on April 14 and ended on April 22. Pre-melt SWE measured on April 10 was 114 mm at the grassland site and 93 mm at the cropland site (Table 4.1). Adding the recorded precipitation during April 10–22 to pre-melt SWE, the amount of water available for runoff was 124 mm for the grassland and 103 mm for the cropland (Table 4.1). Taking the average of two depressions at each site, estimated snowmelt runoff was 37 mm for the grassland and 27 mm for the cropland. Dividing these amounts by available water, the runoff ratio is calculated as 0.30 for the grassland and 0.24 for the cropland, indicating a slightly higher runoff generation at the grassland. Similar calculations for the main runoff event of March 17–27, 2019 gave runoff ratios of 0.59 for the grassland and 0.56 for the cropland. These results indicate that infiltration/runoff characteristics are similar between the grassland and the cropland.

Evapotranspiration (ET) had distinct differences between the grassland and the cropland sites. It started to increase in April at the grassland site (Fig. 4.8a), while it remained low at the cropland site until the crop started to grow vigorously in June (Fig. 4.8b). Wheat (2017 and 2018) and mustard (2019) had higher ET rates than perennial grass during the peak growing season of late June to early August. The wheat ET had a sharp drop around August 12, 2017 and August 15, 2018 as the physiological maturity was reached, whereas mustard had a gradual drop in ET until it reached senescence around September 25, 2019.

Cumulative ET at the grassland had similar seasonal patterns between the three growing seasons (Fig. 4.8c) despite considerable differences in seasonal precipitation patterns (Fig. 4.8e). In contrast, the cumulative ET had different seasonal patterns between wheat (2017 and 2018) and mustard (2019) (Fig. 4.8d). This may indicate the difference in the phenology of the

two crops, or the crop response to higher precipitation in 2019. There were pronounced differences between ET of perennial grass and annual crop during the pre-germination period (May 1–31), when the cropland ET was less than half of the grassland ET (Fig. 4.8f), and during the rapid crop growth (July 1 – August 15), when the cropland ET was 13–46% higher than the grassland ET (Fig. 4.8f). Total ET was much higher than total precipitation during the growing seasons, except for the grassland in 2019, indicating the importance of snowmelt infiltration as a source of soil moisture for vegetative growth.

Cumulative ET at the grassland had similar seasonal patterns between the three growing seasons (Fig. 4.8c) despite considerable differences in seasonal precipitation patterns (Fig. 4.8e). In contrast, the cumulative ET had different seasonal patterns between wheat (2017 and 2018) and mustard (2019) (Fig. 4.8d). This may indicate the difference in the phenology of the two crops, or the crop response to higher precipitation in 2019. There were pronounced differences between ET of perennial grass and annual crop during the pre-germination period (May 1–31), when the cropland ET was less than half of the grassland ET (Fig. 4.8f), and during the rapid crop growth (July 1 – August 15), when the cropland ET was 13–46% higher than the grassland ET (Fig. 4.8f). Total ET was much higher than total precipitation during the growing seasons, except for the grassland in 2019, indicating the importance of snowmelt infiltration as a source of soil moisture for vegetative growth.

Cumulative ET at the grassland had similar seasonal patterns between the three growing seasons (Fig. 4.8c) despite considerable differences in seasonal precipitation patterns (Fig. 4.8e). In contrast, the cumulative ET had different seasonal patterns between wheat (2017 and 2018) and mustard (2019) (Fig. 4.8d). This may indicate the difference in the phenology of the two crops, or the crop response to higher precipitation in 2019. There were pronounced differences between ET of perennial grass and annual crop during the pre-germination period (May 1–31), when the cropland ET was less than half of the grassland ET (Fig. 4.8f), and during the rapid crop growth (July 1 – August 15), when the cropland ET was 13–46% higher than the grassland ET (Fig. 4.8f). Total ET was much higher than total precipitation during the growing seasons, except for the grassland in 2019, indicating the importance of snowmelt infiltration as a source of soil moisture for vegetative growth.

Table 4.1 Pre-melt snow water equivalent (SWE), sum of SWE and precipitation that fell between the snow survey date and the runoff peak date (SWE+P), runoff observed in the first depression (R1: G1 for grass, C1 for crop), runoff observed in the second depression (R2), average runoff (Avg. R), and runoff ratio for the main melt event of 2018 and 2019.

	SWE (mm)	SWE+P (mm)	R1 (mm)	R2 (mm)	Avg. R (mm)	Runoff ratio
			2018			
Grass	114	124	46	28	37	0.30
Crop	93	103	26	23	27	0.24
			2019			
Grass	48	48	36	21	29	0.59
Crop	29	29	17	16	17	0.56

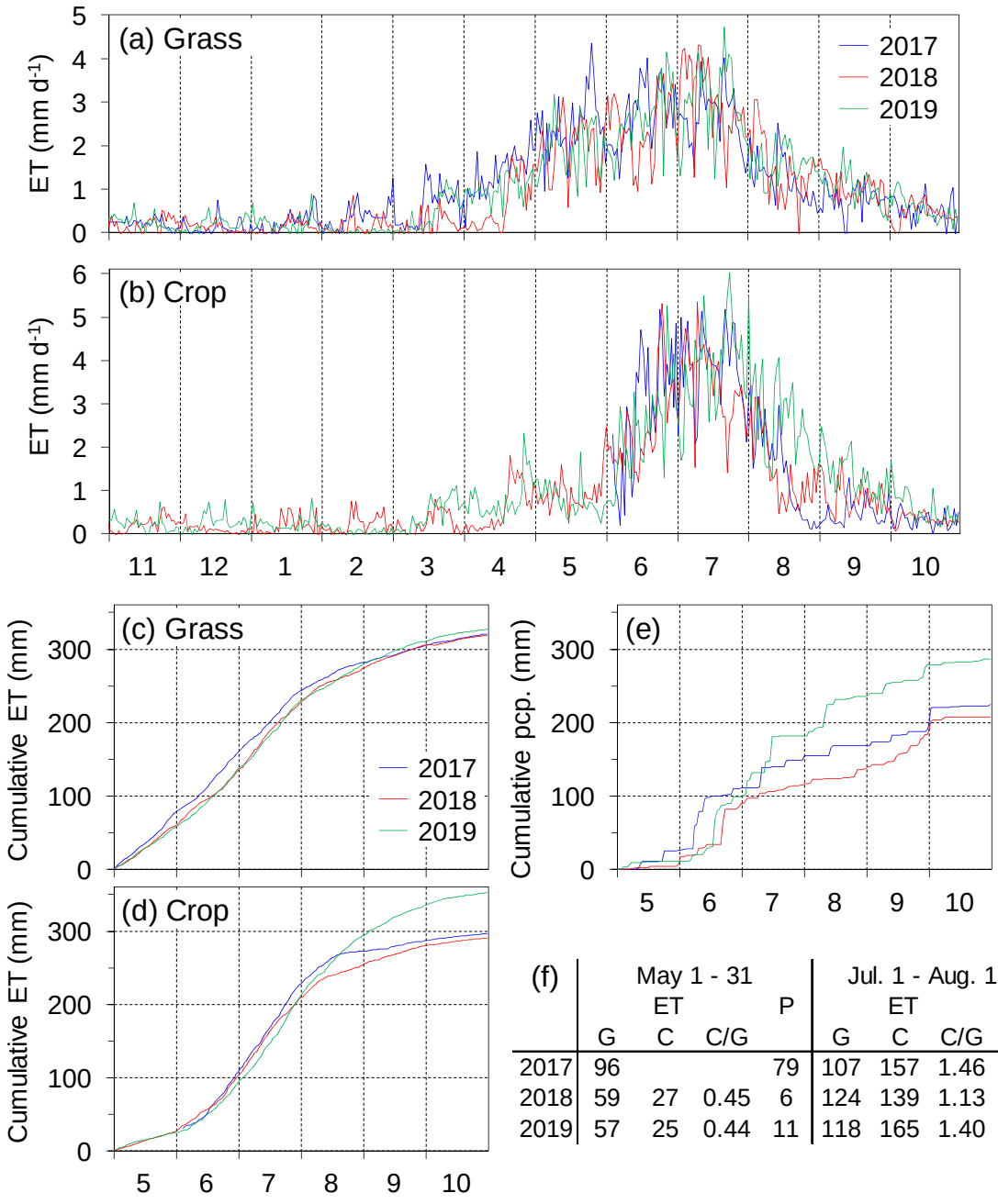

(f)	May 1 - 31				Jul. 1 - Aug. 15			
	ET			P	ET			P
	G	C	C/G		G	C	C/G	
2017	96			79	107	157	1.46	59
2018	59	27	0.45	6	124	139	1.13	39
2019	57	25	0.44	11	118	165	1.40	126

Figure 4.8 (a) Daily average evapotranspiration (ET) fluxes at the grassland site for three hydrological years (November to October). Note that sublimation during winter months is plotted as ET. (b) ET fluxes at the cropland site. (c) Cumulative ET over the growing season (May to October) at the grassland site. (d) Cumulative ET at the cropland site. (e) Cumulative precipitation. (f) Total ET (mm) during May 1 – 31 and July 1 – August 15 at grassland (G) and cropland (C) sites, the ratio of grassland to cropland ET (C/G), and total precipitation (P, mm).

Cumulative ET at the grassland had similar seasonal patterns between the three growing seasons (Fig. 4.8c) despite considerable differences in seasonal precipitation patterns (Fig. 4.8e). In contrast, the cumulative ET had different seasonal patterns between wheat (2017 and 2018) and mustard (2019) (Fig. 4.8d). This may indicate the difference in the phenology of the two crops, or the crop response to higher precipitation in 2019. There were pronounced differences between ET of perennial grass and annual crop during the pre-germination period (May 1–31), when the cropland ET was less than half of the grassland ET (Fig. 4.8f), and during the rapid crop growth (July 1 – August 15), when the cropland ET was 13–46% higher than the grassland ET (Fig. 4.8f). Total ET was much higher than total precipitation during the growing seasons, except for the grassland in 2019, indicating the importance of snowmelt infiltration as a source of soil moisture for vegetative growth.

Chloride concentration in sediment pore water was substantially higher under the uplands than the depressions (Figs. 4.9a and 4.9b), indicating long-term effects of depression-focussed recharge reported in previous studies (e.g., Hayashi et al., 1998; Pavlovskii et al., 2019a). Groundwater tritium concentration was used to differentiate 'modern' (i.e. post-1950) water containing tritium, representing the current land use, and older water representing the pre-agricultural condition for the chloride mass balance analysis. Tritium was detected down to 8 m at the cropland site, whereas groundwater sampled from 6–7 m depth under the grassland did not have detectable tritium (Morgan, 2019). Therefore, average pore-water concentration for the depth zone of 2–5 m is used to represent the C_d of modern water in Eq. (1) for the grassland (Fig. 4.9a), and 2–8 m for the cropland (Fig. 4.9b).

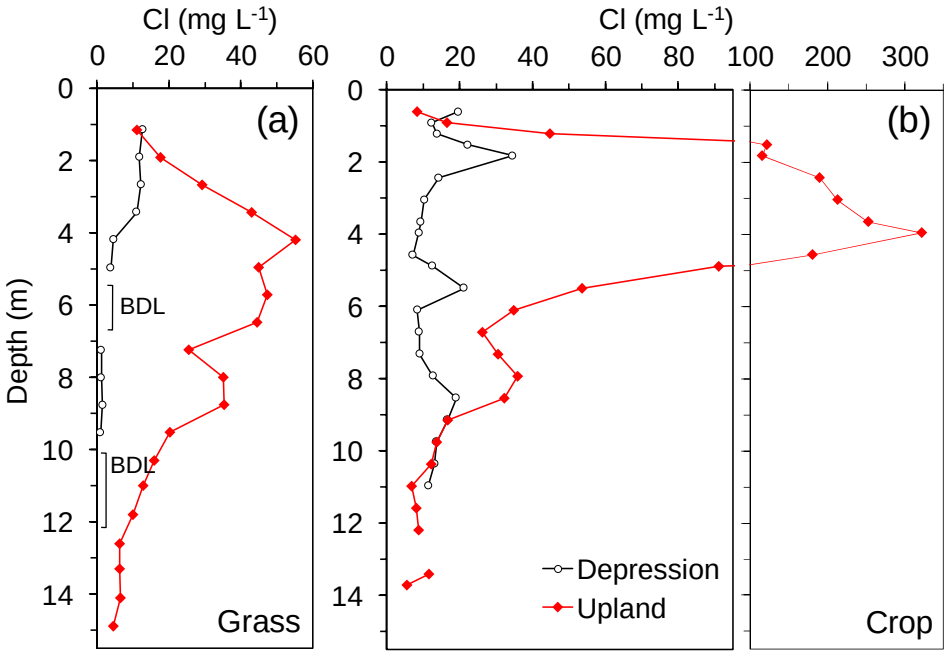

Figure 4.9 (a) Chloride concentration in sediment pore water and groundwater under the depression and the upland at the grassland site. Concentration was below the detection limit (BDL) of 1 mg L^{-1} for some depression samples. Numbers in italic font beside piezometer screens indicate tritium concentration in tritium unit (TU). (b) Chloride concentration at the cropland site.

Table 4.2 Runoff volume collected in the grassland depression G1 and the cropland depression C1, chloride concentration in pond water (C_{pnd}), and estimated lateral transport rates of chloride (Q_{lat}) from the upland to the depression. The data are for the snowmelt period of 2018, 2019, and the average (Avg.) of the two years.

	Runoff volume (m^3)		C_{pnd} (mg L^{-1})		Q_{lat} (mg m^{-2} y^{-1})	
Year	Grass	Crop	Grass	Crop	Grass	Crop
2018	435	278	3.0	3.8	153	111
2019	353	153	5.6	3.9	232	63.6
Avg.	394	216	4.3	3.9	193	86.6

Of the three chloride input terms in Eq. (1), concentration in precipitation (C_p) is estimated to be 0.04–0.07 mg L^{-1} (Pavlovskii et al., 2019a). Multiplying this with mean annual precipitation of 355 mm y^{-1} gives PC_p in a range of 14–25 mg m^{-2} y^{-1}. From the chemical analysis of the fertilizer, the vertical input of chloride (Q_{in}) by fertilizer is estimated to be on the order of 1 mg m^{-2} y^{-1} (Morgan, 2019). Widespread chloride inputs discharged by cattle is estimated to be on the order of 100–200 mg m^{-2} y^{-1} based on the average usage of salt licking blocks (B. Christensen, Triple G Farm, personal communication). Table 4.2 lists Q_{lat} estimated from the runoff volume collected in the ponds in G1 and C1, and the pond chloride concentration. Multiplying these values by A_u/A_d listed in Table 3.2, the lateral chloride input per unit area of the depression ($Q_{lat}A_u/A_d$) ranges 1000–1600 mg m^{-2} y^{-1} in the grassland and 600–1000 mg m^{-2} y^{-1} in the cropland. Compared to these values, PC_p and fertilizer Q_{in} is negligible, and cattle-discharge Q_{in} is likely much smaller than $Q_{lat}A_u/A_d$.

Using the two-year average Q_{lat} (Table 4.2) as the sole input term in Eq. (1), assuming that other terms are negligible, estimated recharge rates (R_d) under the current land use are 150 mm y^{-1} within the grassland depression and 70 mm y^{-1} within the cropland depression. Distributing these over the entire catchment areas (A_c), average recharge rates are 19 mm y^{-1} in the grassland and 7 mm y^{-1} in the cropland with an estimated uncertainty of 2–4 mm y^{-1} (Morgan, 2019).

For the pre-agricultural chloride mass balance under the grassland depression, pore water concentration below 6-m depth was distinctively different from shallower depths, and the corresponding piezometer sample at 5.7–7.2 m had non-detectable tritium. Therefore, the average pore-water concentration for 7–10 m was used to represent C_{gw} of pre-agricultural water in Eq. (2). It was not possible to define the old water concentration under the cropland depression because the deepest pore water samples had similar concentration to the pore water of shallower depths, and sediments from the deeper section of the borehole were not captured by the core tube. Using PC_p of 14–25 mg m^{-2} y^{-1} and C_{gw} = 1.2 mg L^{-1} in Eq. (2), the recharge rate (R_{cat}) in the grassland catchment under the pre-agricultural condition is estimated to be 21 mm y^{-1}.

The paired-catchment study at TG is useful for detailed comparison of hydrological processes, but it has a limited spatial scale. Therefore, snowmelt runoff was estimated for a larger number of depressions in grazed grasslands and croplands using aerial photographs and

satellite images for 2007, 2009, and 2017–2019 (see Morgan, 2019 for detailed methodology). Estimated runoff amounts in croplands were greater in 2017 and 2018 compared to other years (Fig. 4.10). Average runoff in grazed grassland catchments was smaller than in cropland catchments, but the difference was statistically significant ($p < 0.05$) only in 2017 and 2018. This is in contrast to previous studies comparing ungrazed grassland with croplands, reporting substantially lower runoff in ungrazed grassland in Saskatchewan (van der Kamp et al., 2003) and Alberta (Hayashi and Farrow, 2014). Therefore, it seems plausible that the difference in infiltration/runoff characteristics between grazed grassland and cropland is not as pronounced as the difference between ungrazed grassland and cropland.

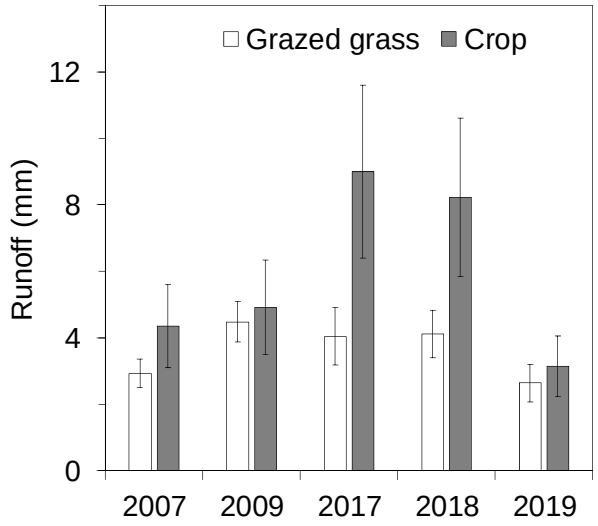

Figure 4.10 Mean snowmelt runoff for the grazed grassland (n = 16) and cropland (n = 12) catchments. Error bars indicate the standard error of mean.

To test the efficacy of VSMB-DUS for differentiating the land-use characteristic between the grazed grassland and the cropland site at Triple G site, the model was set up for both sites and calibrated to minimize the differences between observed and model-simulated hydrological fluxes and soil moisture dynamics. Simulated evapotranspiration fluxes were consistent with observed fluxes (Fig. 4.11). During the three growing seasons (April 1 – October 31), the modeled ET had root-mean-squared error (RMSE) of 0.88 mm d^{-1} and mean bias error (MBE) of -0.14 mm d^{-1} for the grassland site, and RMSE of 0.74 mm d^{-1} and MBE of -0.05 mm d^{-1} for the cropland site. The three-year mean daily evapotranspiration during the growing season was 1.64 mm d^{-1} for both the grassland and the cropland sites. Simulated soil water dynamics captured the seasonal pattern of observed soil water dynamics reasonably well (Fig. 4.12). The RMSE and MBE of the modeled liquid soil water content are listed in Table 4.3 for those soil layers, where observed data were available.

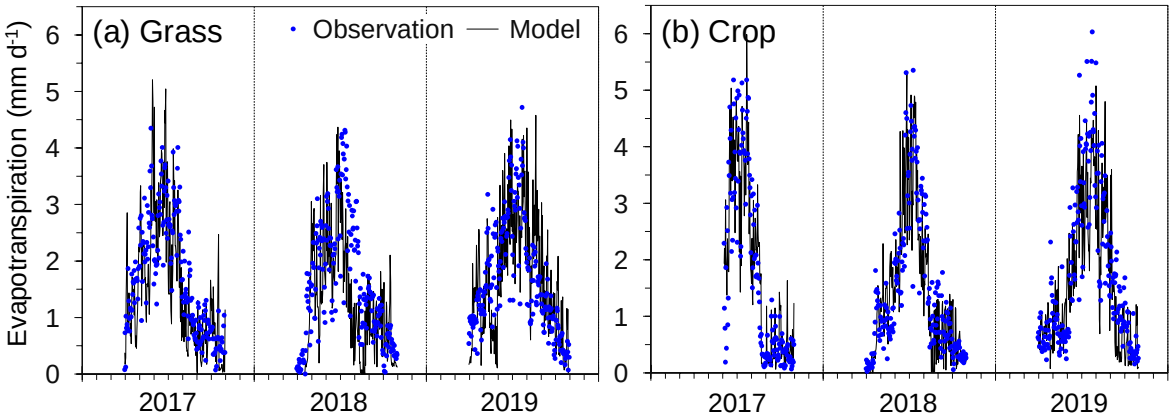

Figure 4.11 Observed evapotranspiration and modelled upland evapotranspiration at (a) grassland site and (b) cropland site during April 1 – October 31 of the three years. Vertical lines indicate January 1 of each year.

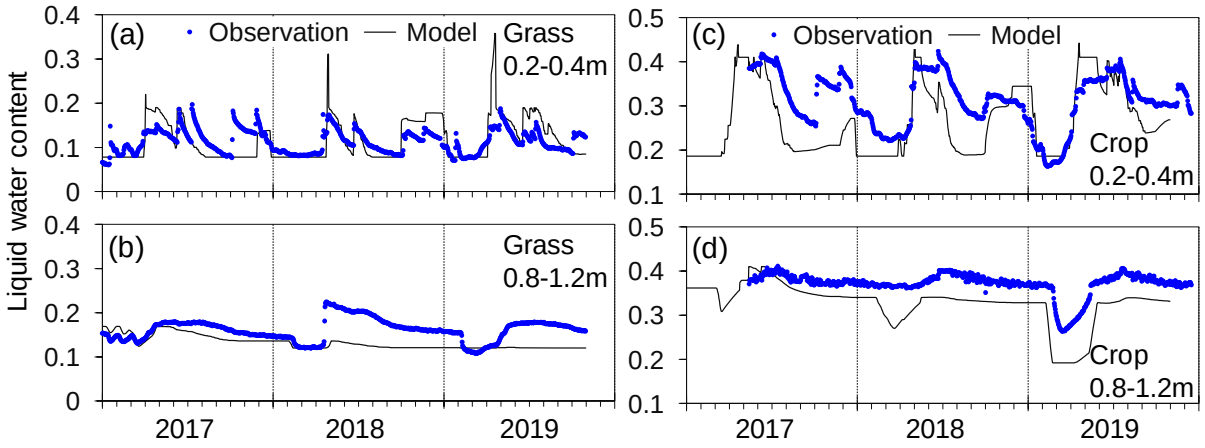

Figure 4.12 Examples of observed and modelled soil liquid water content at upland sites. (a) Grassland in 0.2-0.4m zone. (b) Grassland in 0.8-1.2m zone. (c) Cropland in 0.2-0.4m zone. (d) Cropland in 0.8-1.2m zone. Vertical lines indicate January 1 of each year.

Table 4.3 VSMB model performance statistics for liquid water content at upland locations of the grassland and cropland site; root-mean- squared error (RMSE) and mean bias error (MBE) computed for 2017-2019.

Depth	Grassland		Cropland	
(m)	RMSE	MBE	RMSE	MBE
0.1-0.2	0.09	0.05	0.11	0
0.2-0.4	0.05	0.02	0.09	-0.02
0.4-0.8	0.04	-0.01	0.04	-0.02
0.8-1.2	0.04	-0.02	0.04	-0.03
1.2-2.0	0.06	-0.06	0.01	-0.01

4.3 Effects of irrigation on groundwater recharge

The chloride mass balance (CMB) method (Eq. 1) was applied to estimate groundwater recharge at both the LDF and PP sites using chloride porewater profiles recovered from boreholes drilled at each sub-site. A detailed description is provided in Hughes (2019). Recharge rates at the three depression sub-sites ranged from 88 to 113 mm y^{-1}, which was more than double the rates (29-50 mm y^{-1}) measured at flatland locations (Fig. 4.13). Recharge rates estimated at the upland PP sub-sites were much smaller, with both having values less than 5 mm y^{-1} (Fig. 4.13). When comparing irrigated versus dryland sub-sites, CMB results suggest slightly increased recharge rates on irrigated depressions and flatlands compared to their dryland counterparts, however, topography and landscape position played a much more important role than irrigation status. This is consistent with previous research showing the importance of depression-focused recharge in the prairies and the dominant influence of snowmelt in contributing to groundwater recharge. Note that the CMB recharge rates are a long-term average since irrigation began (40 yr for LDF and 15 yr for PP) and represent point measurements, which are not representative of the average groundwater recharge across the landscape. However, these findings do indicate the importance of small-scale variations in micro-topography at controlling groundwater recharge processes and rates.

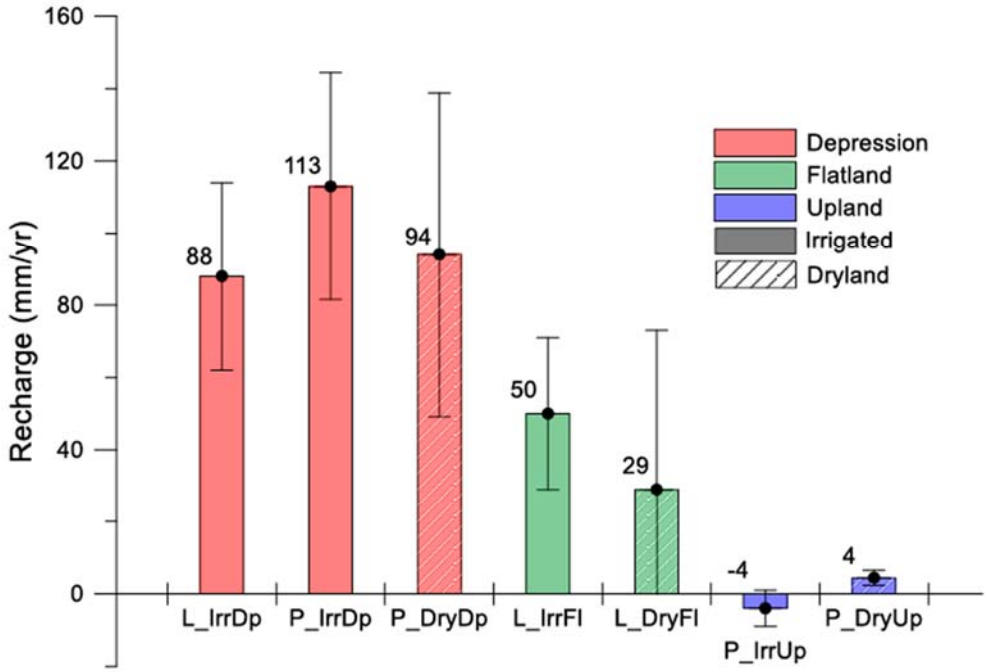

Figure 4.13 Annual recharge rates calculated using the modified chloride mass balance (CMB) method. Error bars represent the uncertainty in recharge estimates.

Figure 4.14 shows the water levels in the two shallowest piezometers from each sub-site at LDF from March to September 2018 (the deep piezometers at L_IrrFl and L_DryFl took months to recover and were therefore omitted). The water table at L_IrrDp (Fig. 4.14a) rose above the ground surface following the March melt event, producing ponding in the depression with a

maximum depth of 0.24 m and reversing the otherwise upward hydraulic gradient for much of the year. Both irrigated and dryland piezometers at flatland sites (Figs. 4.14b and 4.14c) showed an increase in groundwater level around April 19, about one week after the final snowmelt event on April 11. However, only the piezometers at L_IrrFl showed a second increase in water level after July 5, in response to two large irrigation events on July 5 and 6.

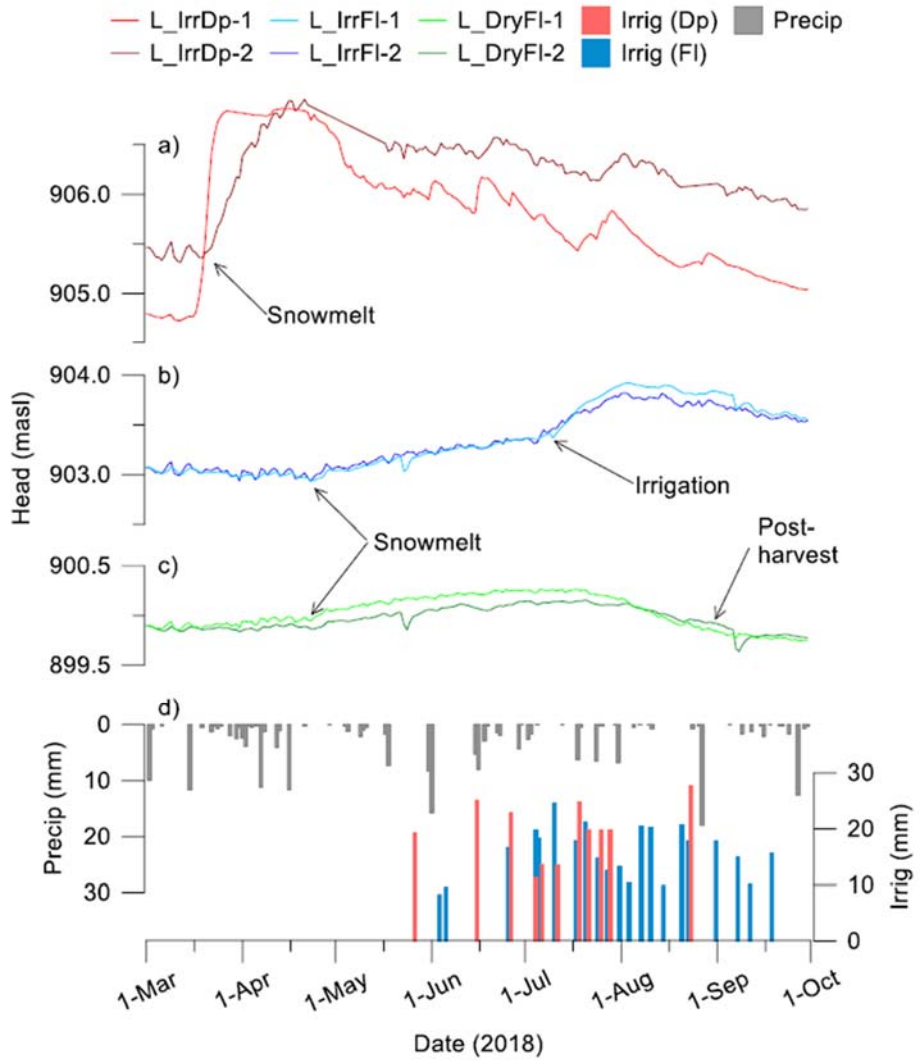

Figure 4.14 Water levels from monitoring wells at LDF at sub-sites L_IrrDp (a), L_IrrFl (b) and L_DryFl (c), along with irrigation and precipitation amounts (d). Arrows indicate the interpreted timing of groundwater responses to snowmelt, irrigation and harvest. Well name suffixes -1 and -2 represent shallower and deeper wells, respectively. Note that wells were sampled on May 23 and September 7 resulting in a perceptible decrease in water level in slow-recovering wells.

The water table fluctuation method (Healy and Cook, 2002) was used to estimate groundwater recharge from the observed water level responses to spring snowmelt and the later response to irrigation, as described above. The recharge calculated from the snowmelt

response in the shallowest well at each sub-site indicated in Fig. 4.14 was 170 ± 34 mm for L_IrrDp and 33 ± 7 mm for both L_IrrFl and L_DryFl. The recharge calculated from the irrigation response at L_IrrFl was 42 ± 9 mm. The estimated recharge in the depression due to snowmelt was nearly five times greater than the corresponding spring recharge at the flatland locations. During the growing season at LDF, the irrigated field (L_IrrFl) had an additional 42 mm of recharge that was attributed to irrigation, meaning summer recharge exceeded the spring recharge amount by about 1.3 times.

Table 4.4 Recharge estimates obtained for all study locations at LDF and PP using different recharge estimation methods. Overwinter/spring season is from November 1, 2017 to April 30, 2018. Summer season is from seeding to harvest 2018. WTF = water table fluctuation method; Wat Bal = water balance method; CMB = chloride mass balance method.

Location	Method	Season	Recharge (mm)
L_IrrDp	WTF	Overwinter	170 ± 34
	Wat Bal	Summer	-39 ± 141*
	CMB	Long term annual	88 ± 26
L_IrrFl	WTF	Overwinter	33 ± 7
	Wat Bal	Overwinter	68 ± 113
	WTF	Summer	42 ± 9
	Wat Bal	Summer	42 ± 141
	CMB	Long term annual	50 ± 21
L_DryFl	WTF	Overwinter	33 ± 7
	Wat Bal	Overwinter	67 ± 113
	Wat Bal	Summer	21 ± 122
	CMB	Long term annual	29 ± 44
P_IrrDp	CMB	Long term annual	113 ± 31
P_IrrUp	CMB	Long term annual	-4 ± 5
P_DryDp	CMB	Long term annual	94 ± 45
P_DryUp	CMB	Long term annual	4 ± 2

*L_IrrDp is a groundwater discharge depression during the summer months

For summer growing season (seeding to harvest) and overwinter/spring (defined as November 1, 2017 to April 30, 2018), recharge amounts were also estimated by completing a water balance using the various measured water inputs, outputs, and changes in water storage in the system (e.g., precipitation, evapotranspiration, runoff, and soil moisture content). Recharge estimates from the water balance method have relatively large uncertainty since the errors are additive, but the relative values can be useful to compare overwinter and growing season periods, as well as serve as a valuable check of the recharge estimates using other methods. A summary of recharge estimates obtained using the water balance approach, along with the previously discussed CMB and WTF methods, at each study location are shown in Table 4.4. Both the water balance and WTF methods showed that overwinter recharge was

nearly identical for both flatlands at LDF, although the water balance method estimated almost double the amount (68 ± 113 and 67 ± 113 mm) compared to the WTF method (33 ± 7 mm). During the growing season at LDF, the water balance and WTF method estimated the same amount of recharge at L_IrrFl (42 ± 9 mm), which was double the amount estimated at L_DryFl using the water balance method (21 ± 122 mm). Note that the water balance method resulted in negative recharge values at L_IrrDp over the summer months, which is consistent with piezometer data (Fig. 4.14a) that indicated an upward hydraulic gradient during this period.

Results from all methods at both LDF and PP study sites show that, regardless of irrigated or dryland conditions, groundwater recharge rates were greatest beneath depressions, moderate beneath flatlands and very low (if any) beneath uplands (Table 4.4). Topographically driven depression-focused groundwater recharge behaviour observed at other prairie sites is important even in relatively very low relief glacial sediments, such as those at the LDF site. Additionally, stable isotope data collected at both LDF and PP sites further support the hypothesis that snowmelt is the dominant source of recharge in topographical lows (not shown; Hughes, 2019). As such, snowmelt is likely the dominant source of recharge on dryland fields and is also important on many irrigated fields. Nevertheless, irrigation practices still contribute to an increase in groundwater recharge over the growing season, especially in flatland situations like the LDF site. All three recharge estimation methods at the LDF site showed the irrigated flatland field (L_IrrFl) had higher summer or annual recharge rates in comparison to the dryland field site (L_DryFl)(Table 4.4). The exact magnitude of the irrigation influence is difficult to quantify based on differences and limitations of the various methods, however, the contribution of irrigation to summer recharge is expected to be 2–3 times the amount in dryland fields.

The VSMB upland model was used to simulate the soil moisture dynamics under the dryland (L_DryFl) and the irrigated (L_IrrFl) sites. The model captured the seasonal pattern of soil moisture dynamics during the 2018 growing season reasonably well (Fig. 4.15). The soil under the irrigated field maintained high moisture contents, whereas the soil under the dryland became drier in August.

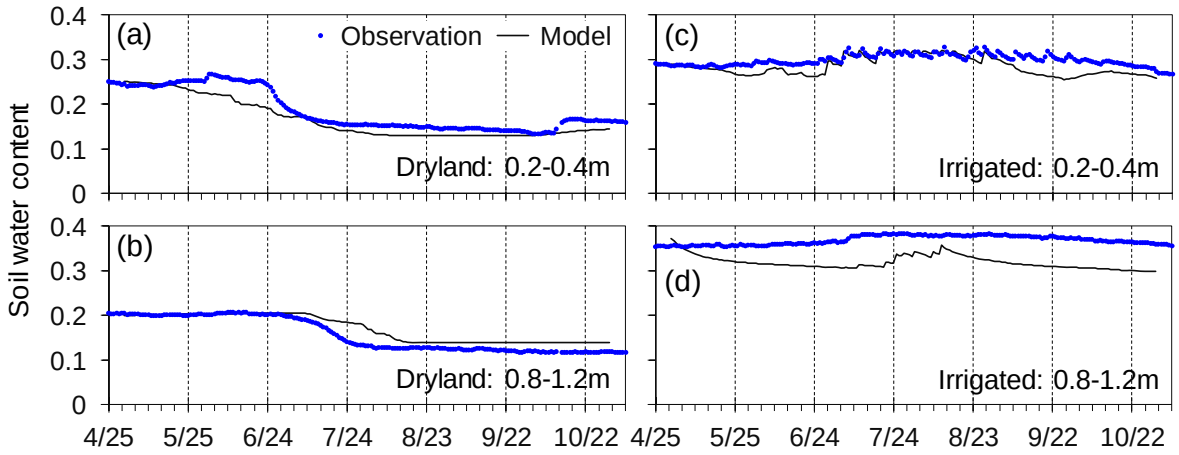

Figure 4.15 Examples of observed and modelled soil liquid water content at Lethbridge site during 2018 growing season. (a) Dryland site (L_DryFl) in 0.2-0.4m zone. (b) Dryland site in 0.8-1.2m zone. (c) Irrigated site (L_IrrFL) in 0.2-0.4m zone. (d) Irrigated site in 0.8-1.2m zone.

4.4 Watershed-scale comparison of model recharge and stream baseflow

The results of groundwater recharge simulation using VSMB-DUS (Fig. 4.5c) were used with the groundwater flow model of the West Nose Creek watershed. Daily recharge outputs from VSMB-DUS were used as the surface boundary condition for the flow model (Abdrakhimova, 2020). Of the 11 monitoring wells in the watershed, six showed clear seasonal water level fluctuations in response to recharge events. Following the method of Hayashi and Farrow (2014), the observed magnitude of annual water level rise in monitoring wells (see Fig. 4.5c for location) was compared against the simulated annual recharge at the same locations (Fig. 4.16). The moderate correlation between water level rise and recharge at most locations suggest that VSMB-DUS captures the interannual variability of recharge reasonably well. This is consistent with the results in Section 4.1 comparing the interannual variabilities of simulated recharge and observed creek baseflow (Fig. 4.5a).

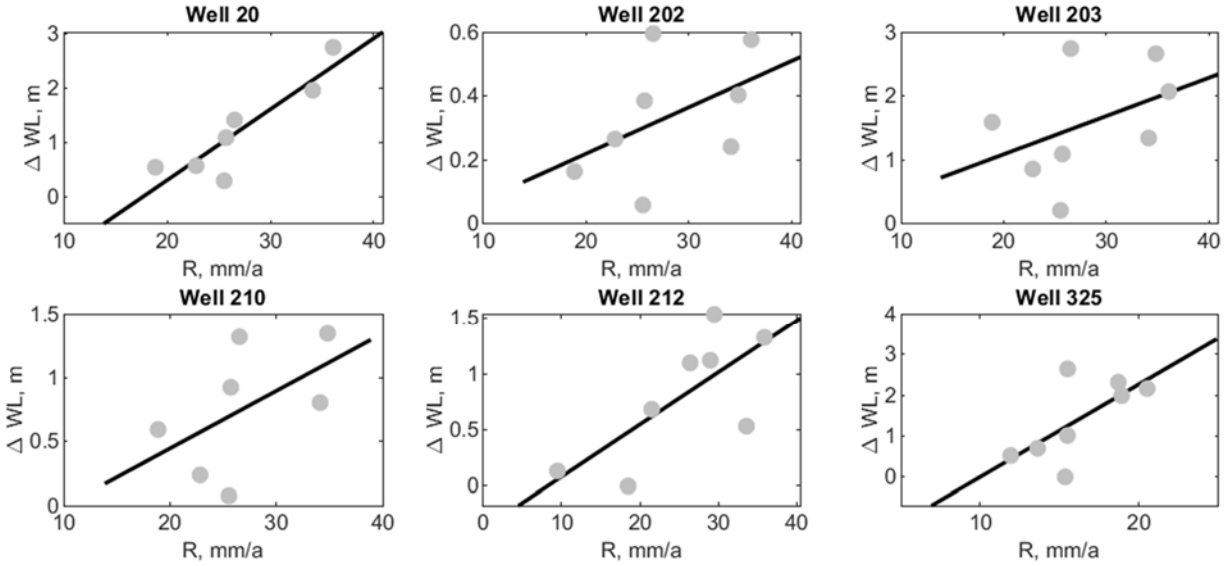

Figure 4.16 Cross-plots of modeled annual recharge (R, mm y^{-1}) and seasonal water level increase ΔWL (m) derived from the measured water levels in observation wells.

Using the same groundwater flow model of the West Nose Creek watershed, a solute transport simulation was conducted to characterize the residence time of water in the aquifers. A reverse particle tracking method was used to simulate the pathways and transit times of water captured by the pumping wells in the model domain. Estimated transit times may not provide accurate residence time of groundwater due to the large uncertainty in aquifer parameters, but they offer qualitative insights into the distribution of residence time within the watershed. The simulation results showed that the water captured by pumping wells was recharged in the local vicinity for most of the wells, and only those wells located close to the water courses had water originating in distant recharge areas (Fig. 4.17). Over 80% of wells had simulated water residence time of 100 years or longer.

To compare simulation results with actual residence time of groundwater, water samples were collected from nine wells in the watershed and analyzed for tritium concentration. Tritium

(^{3}H) is a radioactive isotope of hydrogen (^{1}H) and has a half life of 12.7 years. Presence of tritium in a water sample indicates that at least a part of the water is sourced by post-1950 precipitation. Seven out of nine wells had detectable amounts of tritium (Table 4.5), suggesting that the groundwater from these wells contained post-1950 water. Noting that the recharge flux in the groundwater model is distributed over the entire landscape, whereas actual recharge is focussed under depressions occupying a small fraction (typically < 5%) of the landscape, the vertical flow velocity of groundwater under depressions is expected to be much higher than the land-scape average recharge rate. This may explain the shorter residence time indicated by tritium compared to groundwater model simulation. Further study is required to understand the tracer transport processes associated with depression-focussed recharge.

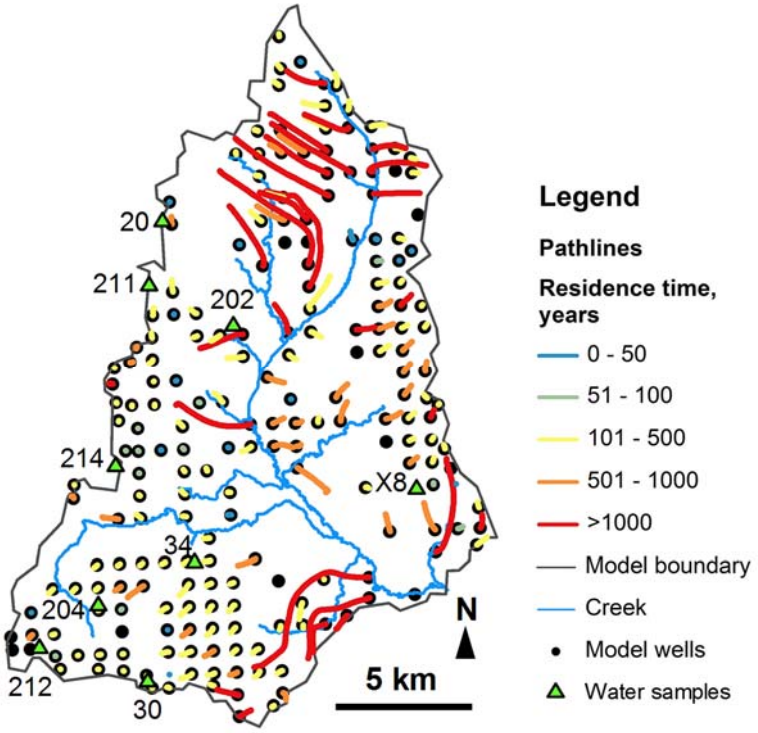

Figure 4.17 Simulated flow path lines and residence times of groundwater captured by pumping wells in the West Nose Creek watershed. The map also indicates the location of wells, from which water samples were collected for tritium analysis.

Table 4.5 Tritium (^{3}H) concentration in water samples collected from the wells in the West Nose Creek watershed. Well IDs correspond to those in Rocky View Well Watch network, except for X8. Depth indicates the middle depth of the well screen.

Well ID	Depth (m)	^{3}H (TU)	Well ID	Depth (m)	^{3}H (TU)
20	32.8	7.5	211	13.7	9.1
30	42.7	2.4	212	35.1	4.9
34	91.4	1.2	214	27.1	6.3
202	36.6	< 0.8	X8	32.0	6.8
204	60.2	< 0.8			

4.5 Potential effects of climate change

Outputs of meteorological variables by the WRF model represents a climate scenario for hydrological years 2092-2100 under the pseudo global warming (PGW) condition. The WRF model was forced by an assemble of 19 GCMs, which were in turn forced by the emission scenario of representative concentration pathway representing the 'business as usual' scenario (RCP8.5). The WRF outputs were corrected for biases in air temperature and precipitation by comparing the modeled and observed variables for HY 2007–2015 at the Spyhill site (Fig. 4.18) as described in Section 3.5. The climate under PGW scenario in HY 2092-2100 was warmer and wetter than the historical observations in HY2007–2015 at the Spyhill site (Fig. 4.19).

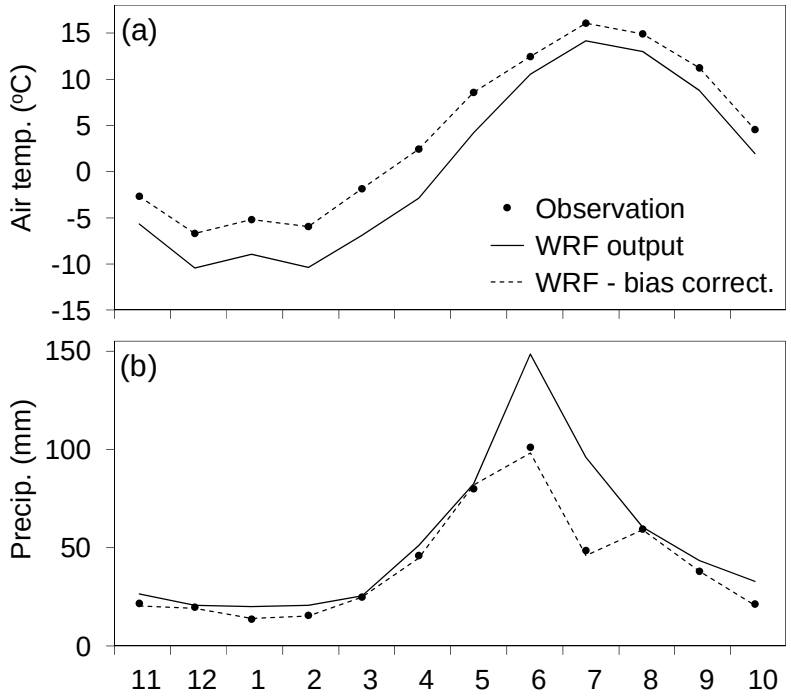

Figure 4.18 (a) Monthly mean air temperature and (b) monthly total precipitation averaged over HY2007−2015, observed at the Spyhill site and modeled by WRF. The biases between WRF outputs and observations were corrected by the bivariate quantile mapping method.

The bias-corrected WRF outputs were used with VSMB-DUS to simulate groundwater recharge under the PGW scenario. Simulated groundwater recharge decreased under the PGW scenario except for HY2099–2100 (Fig. 4.3). High recharge values in these two years was a result of continuous ponding of the depressions from August to March caused by the extremely high runoff in August 2099. Over-winter ponding in these depressions was never observed under the present climate. Average recharge over the simulation period decreased from 6.2 mm y^{-1} under the present climate to 3.6 mm y^{-1} under the PGW.

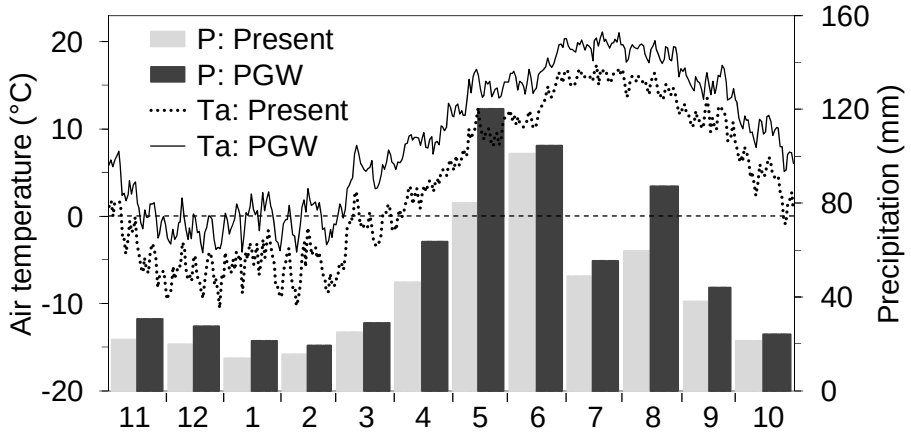

Figure 4.19 Mean monthly precipitation (P) and daily air temperature (Ta) observed at the Syphill site during HY2007−2015 and simulated by WRF under the pseudo global warming (PGW) scenario for HY2092−2100 with bias correction.

To assess the regional-scale effects of climate change, the bias-corrected WRF outputs were prepared for the 37 meteorological stations (Fig. 3.5), and used with VSMB-DUS to simulate groundwater recharge for HY2095-2100 under the PGW. The spatial pattern and magnitude of simulated recharge under the PGW (Fig. 4.20) were similar to those of simulated recharge under the present climate (Fig. 4.6). The PGW recharge rates mostly ranged 5-60 mm y^{-1} for grassland and 5-70 mm y^{-1} for cropland (Fig. 4.20). Recharge rates increased slightly in the northern parts of the region characterized by wetter and colder climate, and decreased slightly in the southern parts (Fig. 4.21). However, it should be noted that the comparison period covers HY2010-2015 (present) and HY2095-2100 (PGW), which included the years of high recharge under PGW (HY2099-2100) caused by extremely high runoff in August 2009 (Fig. 4.3). The increase in recharge under PGW is likely biased by the high recharge during HY2099-2100.

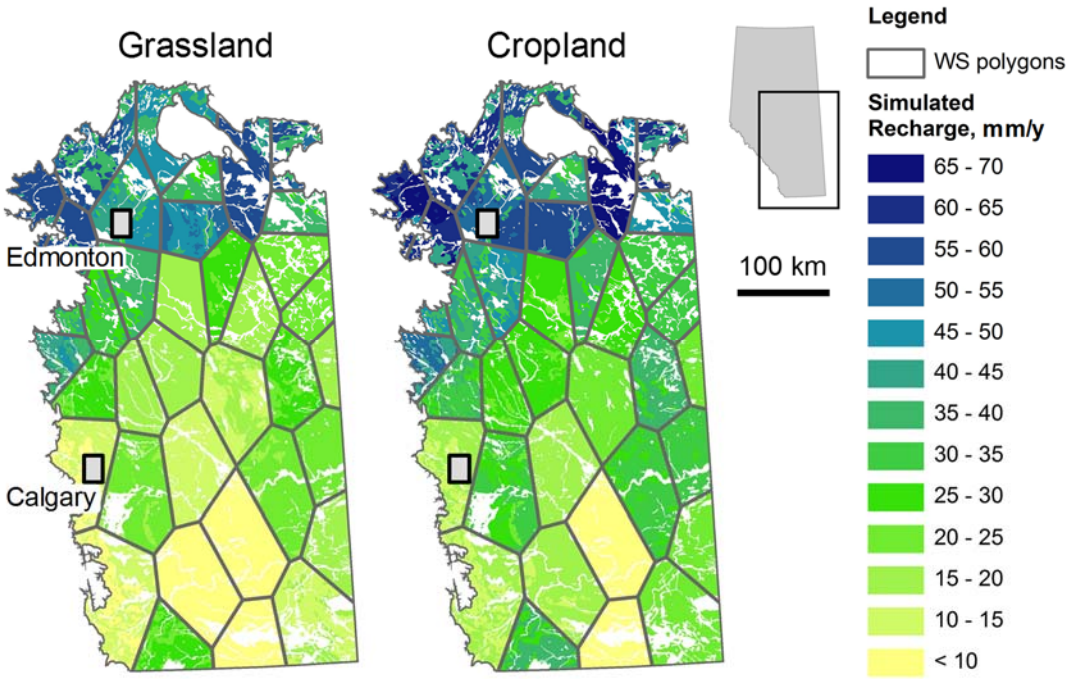

Figure 4.20 Distribution of average groundwater recharge rates under the pseudo global warming scenario during HY2095-2100 simulated by VSMB-DUS in the agricultural regions of central and southern Alberta.

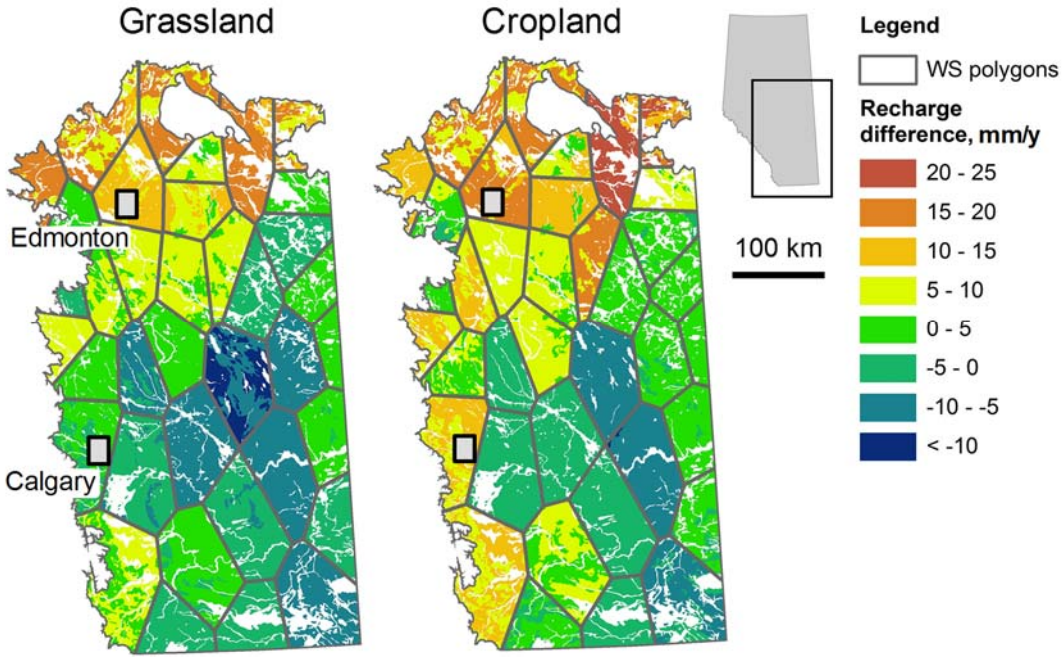

Figure 4.21 Difference in simulated groundwater recharge between HY2010-2016 (present climate) and HY2095-2100 (pseudo global warming scenario). Positive values indicate increases in recharge under the warming scenario.

4.6 Discussion of project metrics and variances

The project deliverables were described in the project proposal as a series of research tasks (Table 4.6). All tasks were completed during the study. Other key metrics are: 1) dissemination of research results at conferences and in scientific publications, 2) training of highly qualified and skilled personnel (HQSP), and 3) transfer of knowledge to potential user groups. These metrics are discussed in Sections 6 and 7.

Table 4.6 Project tasks and their achievement status

	Task description	**Status**	**Remarks**
Task 1	Spatial variability of recharge processes		
1.1	Expansion of study sites	Complete	All sites established.
1.2	Observation and model testing	Complete	Three full seasons of field data collected.
1.3	Testing of up-scaling methods	Complete	Upscaling method has been established.
Task 2	Hydrologic effects of land-use practices		
2.1	Land-use manipulation	Complete	Paired-plot experiment completed.
2.2	Recharge model modification	Complete	Model parameters calibrated using archived data from multiple land-use sites.
Task 3	Soil moisture dynamics and groundwater recharge under irrigated fields		
3.1	Site establishment	Complete	Site established and decommissioned after the completion of data collection.
3.2	Hydrological fluxes observation	Complete	Two full seasons of flux data collected.
3.3	Recharge model testing	Complete	Recharge model applied to the LDF sites.
Task 4	Watershed-scale validation of the recharge model		
4.1	Watershed water balance	Complete	Comparison of watershed recharge and baseflow completed.
4.2	Groundwater flow model	Complete	Model established using FEFLOW.
4.3	Residence time analysis	Complete	Residence time computed by FEFLOW and compared with tritium data.
Task 5	Climate change impacts		
5.1	Downscaling methodology	Complete	Downscale complete using the WRF model, and outputs bias-corrected.
5.2	Climate scenario development	Complete	PGW scenario developed.
5.3	Impacts assessment	Complete	Recharge maps prepared for PGW scenario.

5. KEY LEARNINGS

The project has generated a body of knowledge that advances our understanding of groundwater recharge processes in the Edmonton-Calgary-Lethbridge Corridor and the agricultural areas of Alberta in general. While detailed results are described in Section 4, the key outcomes are the following.

(1) Depression-focussed recharge is the predominant mode of recharge under the present climate both in grasslands and croplands of Alberta. Therefore, recharge amounts can be strongly influenced by changes in the transfer of snow-derived water from uplands to depression as a result of land management practices.
(2) Grazed grasslands and croplands have similar runoff characteristics, despite having dissimilar plant phenology and evapotranspiration characteristics. This suggests that depression-focussed recharge is not influenced by agricultural land use alone. It is important to consider the combined effects of land use and topography.
(3) Irrigation results in an increased groundwater recharge compared to dryland cropping. However, depression-focussed recharge remains the dominant mode of recharge in irrigated fields, even in relatively flat terrain.
(4) Depression-focussed recharge will persist under the future climate in Alberta, though the amount may decrease slightly and the timing may shift from spring to summer.
(5) Regional-scale recharge rates range from 5 to 60 mm y^{-1} in the agricultural region of Alberta. This puts a constraint on long-term pumping rates from shallow aquifers (< 100 m) in the region.

6. OUTCOMES AND IMPACTS

6.1 Groundwater recharge model

An important outcome of the project is the groundwater recharge model (VSMB-DUS) specifically developed for the estimation of depression-focussed recharge in the Canadian prairies. The model has been tested at instrumented study sites under various land-use conditions, namely ungrazed grass, grazed grass, alfalfa field, annual crop (dryland), and annual crop (irrigated). The statistical upscaling methodology has been developed to estimate recharge over a large scale, which is useful for estimating recharge in the agricultural region of Alberta (see 6.2 below). This outcome corresponds to the deliverables of Tasks 1, 2, and 3.

6.2 Groundwater recharge map

Using VSMB-DUS and the statistical upscaling methodology, long-term average values of groundwater recharge were estimated for the agricultural region of central and southern Alberta including the Edmonton-Calgary-Lethbridge Corridor for the two most common land-use types, namely grazed grassland and croplands. The results were validated against long-term baseflow data in watersheds where reliable data were available. This information is useful for evaluating sustainable rates of groundwater extraction at various scales under the present

climate and land use. Recharge amounts were also estimated for the same region under a climate warming scenario. This outcome corresponds to the deliverables of Tasks 4 and 5.

6.3 Project outputs

6.3.1 Journal articles

Mohammed, A.A., Cey, E.E., Hayashi, M., Callaghan, M.V., Park, Y-.J., Miller, K.L. and Frey, S.K. 2021. Dual-permeability modeling of preferential flow and snowmelt partitioning in frozen soils. Vadose Zone Journal (in press).

Mohammed, A.A., Kurylyk, B.L., Cey, E.E. and Hayashi, M. 2018. Snowmelt infiltration and macropore flow in frozen soils: overview, knowledge gaps and a conceptual framework. Vadose Zone Journal, 17: 180084.

Mohammed, A.A., Pavlovskii, I., Cey, E.E. and Hayashi, M. 2019. Effects of preferential flow on snowmelt partitioning and groundwater recharge in frozen soils. Hydrology and Earth System Sciences, 23, 5017–5031.

Noorduijn, S.L., Hayashi, M., Mohammed, G.A. and Mohammed, A.A. 2018. A coupled soil water balance model for simulating depression-focused groundwater recharge. Vadose Zone Journal, 17: 170176.

Pavlovskii, I., Hayashi, M. and Itenfisu, D. 2019. Effects of midwinter snowmelt on runoff generation and groundwater recharge in the Canadian prairies. Hydrology and Earth System Sciences, 23: 1867-1883.

Pavlovskii, I., Hayashi, M. and Cey, E.E. 2019. Estimation of depression-focussed groundwater recharge using chloride mass balance: Problems and solutions across scales. Hydrogeology Journal, 27: 2263-2278.

Pavlovskii, I., Hayashi, M. and Lennon, M.R. 2018. Transformation of snow isotopic signature along groundwater recharge pathways in the Canadian Prairies. Journal of Hydrology, 563: 1147-1160.

Pavlovskii, I., Noorduijn, S.L., Liggett, J.E., Klassen, J. and Hayashi, M. 2020. Quantifying terrain controls on runoff retention and routing in the Northern Prairies. Hydrological Processes, 34: 473-484.

Pittman, F., Mohammed, A. and Cey, E. 2020. Effects of antecedent moisture and macroporosity on infiltration and water flow in frozen soil. Hydrological Processes, 34:795–809.

Copies of the above articles are included as the attachment to this report.

6.3.2 Student theses

Abdrakhimova, P. 2020. Improving groundwater flow model parameterization techniques. Ph.D. Thesis, University of Calgary.

Hughes, A.T. 2019. Investigating groundwater recharge rates and seasonality under irrigated and dryland conditions at two agricultural sites near Lethbridge, Alberta. M.Sc. Thesis, University of Calgary.

Mohammed, A.A. 2019. Measurement and simulation of preferential flow in frozen soils. Ph.D. Thesis, University of Calgary.

Morgan, L.R. 2019. Land use effects on depression-focussed groundwater recharge in the prairies. M.Sc. Thesis, University of Calgary.
Muenchrath, A.K. 2019. Land-use and topographic effects on near-surface saturated hydraulic conductivity and soil properties in southern Alberta. B.Sc. Thesis, University of Calgary.
Pavlovskii, I. 2019. Groundwater recharge in the prairies: mechanisms, constraints, and rates. Ph.D. Thesis, University of Calgary.

6.3.3 Technical reports

Klassen, J., Liggett, J.E., Pavlovskii, I., and Abdrakhimova, P. 2018. First-order groundwater availability assessment for southern Alberta. Alberta Energy Regulator / Alberta Geological Survey. AER/AGS Open File Report 2018-09. 37pp.

6.3.4 Conference presentations (listed in chronological order)

Abdrakhimova, P., Bentley, L.R. and Hayashi, M. 2017. Numerical simulation of long-term pumping in a heterogeneous sandstone aquifer. International Association of Hydrogeologists Symposium on Characterizing Regional Groundwater Flow System. Calgary, June 27-28.
Felske, A., Cey, E.E. and Hayashi, M. 2017. Evaluating groundwater-surface water interactions at a large permanently flooded wetland in the Canadian prairies. International Association of Hydrogeologists Symposium on Characterizing Regional Groundwater Flow System. Calgary, June 27-28.
Hayashi, M., Abdrakhimova, P., Niazi, A., Bentley, L.R. and Cey, E.E. 2017. Meaning of recharge in the context of regional groundwater management framework: Alberta example. International Association of Hydrogeologists Symposium on Characterizing Regional Groundwater Flow System. Calgary, June 27-28.
Mohammed, A., Cey, E.E. and Hayashi, M. 2017. Vadose zone dynamics governing snowmelt infiltration and depression-focused recharge in prairie landscapes. International Association of Hydrogeologists Symposium on Characterizing Regional Groundwater Flow System. Calgary, June 27-28.
Niazi, A., Bentley, L.R. and Hayashi, M. 2017. Conditioning the geostatistical simulation of Paskapoo formation with lithologs, paleo-current statistics and pumping test for stochastic regional groundwater modeling. International Association of Hydrogeologists Symposium on Characterizing Regional Groundwater Flow System. Calgary, June 27-28.
Pavlovskii, I., Lennon, M.R. and Hayashi, M. 2017. Depression-focussed recharge in the prairies of Alberta: Insights from stable isotope data. International Association of Hydrogeologists Symposium on Characterizing Regional Groundwater Flow System. Calgary, June 27-28.
Rasouli, K., Krogh, S., Pavlovskii, I., Hayashi, M. and Pomeroy, J.W. 2017. The role of soil freezing and thawing in hydrological processes: Canadian case studies. The 2nd Asian Conference of Permafrost, Sapporo, Japan, July 2-6.
Cey, E.E., Felske, A. and Hayashi, M. 2017. Water and chloride mass budgets of a permanently flooded, seasonally frozen wetland in the Canadian prairies. Annual Meeting of Geological Society of America, Seattle, Washington, October 22-25.
Rasouli, K., Pomeroy, J.W., Hayashi, M., Fang, X., Gutmann, E.D., and Li, Y., 2017. Assessment of the suitability of high resolution numerical weather model outputs for hydrological

modelling in mountainous cold regions. Fall Meeting of the American Geophysical Union. New Orleans, Louisiana, December 11-15.
Abdrakhimova, P., Bentley, L.R., and Hayashi, M. 2018. Delineation of a sandstone channel in a heterogeneous aquifer from well tests and geophysical data using an optimization algorithm. The 45th Congress of the International Association of Hydrogeologists, Deajeon, Korea, September 9-14.
Hughes, A., Cey, E.E., and Hayashi, M. 2018. The role of irrigation in depression-focused groundwater recharge in the Canadian Prairies. Joint Annual Meeting of the Canadian Geotechnical Society and the International Association of Hydrogeologists - Canadian National Chapter. Edmonton, Alberta, September 23-26.
Morgan, L.R., Hayashi, M., Negm, A., Cey, E.E. 2018. Land-use effects on depression-focussed groundwater recharge in the prairies: Water balance approach. Joint Annual Meeting of the Canadian Geotechnical Society and the International Association of Hydrogeologists - Canadian National Chapter. Edmonton, Alberta, September 23-26.
Negm, A., Hayashi, M., Itenfisu, D. 2018. Comparison of root water uptake and soil moisture dynamics under contrasting land uses in the Canadian Prairies. Joint Annual Meeting of the Canadian Geotechnical Society and the International Association of Hydrogeologists - Canadian National Chapter. Edmonton, Alberta, September 23-26.
Pavlovskii, I., Hayashi, M. 2018. Pitfalls in groundwater recharge evaluation using chloride mass balance in the Canadian Prairies. Joint Annual Meeting of the Canadian Geotechnical Society and the International Association of Hydrogeologists - Canadian National Chapter. Edmonton, Alberta, September 23-26.
Abdrakhimova, P., Bentley, L.R., Hayashi, M. 2018. Hydrogeological factors affecting seasonal fluctuations of groundwater levels in a heterogeneous bedrock aquifer. Joint Annual Meeting of the Canadian Geotechnical Society and the International Association of Hydrogeologists - Canadian National Chapter. Edmonton, Alberta, September 23-26.
Rasouli, K., Negm, A., Pavlovskii, I., Pomeroy, J.W., Hayashi, M. 2018. Surficial geology-based mapping of the future changes in groundwater recharge in a semi-arid watershed in the Canadian Prairies with climate warming. Fall Meeting of the American Geophysical Union, Washington D.C., December 10-14.
Muenchrath, A., and Cey, E. 2019. Land use and topographic effects on near-surface saturated hydraulic conductivity and soil properties in southern Alberta. Geoscience Research Exchange (GeoREX), Calgary, Alberta, April 4.
Cey, E., Mohammed, A., Pittman, F. and Hayashi, M. 2019. Infiltration, groundwater recharge and preferential flow dynamics in frozen ground. Joint Conference of GAC-MAC and International Association of Hydrogeologists-Canadian National Chapter, Quebec, Quebec, May 12-15.
Khawaja, S., Pittman, F. Morgan, L., Mohammed, A.A., Hayashi, M. and Cey, E.E. 2020. Understanding and quantifying effects of midwinter melt events on preferential flow in frozen prairie soils. Canadian Geophysical Union Seminar Series, June 26, 2020, Virtual.
Abdrakhimova, P., Bentley, L.R. and Hayashi, M. 2020. Factors affecting seasonal response of groundwater levels to depression-focused recharge in bedrock wells. GeoConvention 2020, September 21-23, Virtual.

Khawaja, S., Pittman, F., Morgan, L., Mohammed, A., Hayashi, M. and Cey, E. 2020. Field and laboratory analysis of snowmelt partitioning and quantification of preferential flow in frozen prairie soils. GeoConvention 2020, September 21-23, Virtual.

Negm, A., Rasouli, K. and Hayashi, M. 2020. Climate-change effects on groundwater recharge in the prairies. GeoConvention 2020, September 21-23, Virtual.

7. BENEFITS

7.1 Economic benefits

The VSMB-DUS model is a versatile tool to simulate soil moisture conditions in agricultural lands and to estimate depression-focussed groundwater recharge. Due to its relatively simple numerical algorithms and small data requirements, the model has the potential to be adopted by non-academic users. For example, it can be used to estimate groundwater recharge rates for industrial applications such as modelling studies of contaminant remediation or water supply evaluation. Another example is agricultural application, where the upland module of VSMB-DUS can be used to simulate soil moisture conditions in croplands or grass pastures. These and other model applications will provide economic benefits to environmental and agricultural sectors.

7.2 Environmental benefits

Groundwater availability assessment in Alberta has conventionally relied on well-based approaches, whereby pumping tests are used to estimate permissible rates of groundwater extraction. However, potential deficiencies of the well-based approach have been identified by previous reports (e.g., Maathuis and van der Kamp, 2006). The water balance approach offers a viable and more holistic alternative, but it requires reliable estimates of groundwater recharge. The VSMB-DUS model provides a reliable tool for recharge estimation in the unique environment of the Canadian prairies, where recharge is focussed under depressions. Using the water balance approach for groundwater availability assessment, it is now possible to consider the effects of groundwater extraction on spring discharge and stream baseflow, and groundwater dependent ecosystems. The new approach will aid the development of Groundwater Management Framework (see below) in Alberta and provide important environmental benefits.

7.3 Social benefits

The project has strengthened stakeholder involvement through close collaboration with Alberta Energy Regulator / Alberta Geological Survey (AER/AGS), Alberta Environment and Parks (AEP), and Alberta Agriculture and Forestry (AF). The VSMB-DUS model was used by AER/AGS to produce a first-order assessment of groundwater availability in Alberta (Klassen et al., 2018). Two project investigators (Hayashi and Cey) assisted AEP in formulating the new Groundwater Management Framework for Alberta. AF provided the data from the network of agricultural meteorological stations for the development and testing of VSMB-DUS, and also provided access to Lethbridge Demonstration Farm for the irrigation study.

7.4 Building innovation capacity

7.4.1 Highly qualified and skilled personnel (HQSP)

The project has trained the following individuals, who obtained meaningful employment in industrial and academic sectors (indicated in brackets).

Amro Negm, postdoctoral fellow (University of Calgary, postdoctoral fellow)
Igor Pavlovskii, PhD (Dalhousie University, postdoctoral fellow)
Aaron Mohammed, PhD (Dalhousie University, postdoctoral fellow)
Polina Abdrakhimova, PhD (CBCL Ltd., hydrogeologist)
Alexandra Hughes, MSc (BGC Engineering Inc., hydrogeologist)
Laura Morgan, MSc (Parsons Corp., hydrogeologist)
Alana Muenchrath, BSc (University of Saskatchewan, MSc student)
Brandon Hill, field technician (Applied Aquatic Research Ltd., hydrologist)
Evan Sieben, field technician (BGC Engineering Inc., hydrogeologist)

7.4.2 Research infrastructure

The research infrastructure for long-term monitoring at the West Nose Creek hydrological observatory has been enhanced during the project with replacement and repair of aging sensors. The observatory has been operating since 2003 with comprehensive monitoring systems for land-atmosphere exchange, surface water, and subsurface water. The infrastructure is being used in a new AI-WIP project, 'Assessing hydrological connectivity in rural and urban watersheds for improved water management' (Principal Investigator: Edwin Cey).

8. RECOMMENDATIONS AND NEXT STEPS

This project developed a new tool to estimate groundwater recharge in the unique environment of the Canadian prairies. The new tool was used to produce recharge estimates for the agricultural regions of central and southern Alberta. The recharge values represent the amount of water added to the water table, which may or may not be located in aquifers used for water supply. Therefore, it is important to understand the connection between the water-table recharge and the recharge of deeper aquifers induced by pumping. This topic is being investigated in a separate project, Prairie Water (https://gwf.usask.ca/prairiewater/) funded by Global Water Futures program.

The new information on groundwater recharge can be implemented in a watershed-based groundwater management to assess the availability of groundwater resources. The conceptual basis for the new Groundwater Management Framework is being explored by Alberta Environment and Parks (AEP), and the information generated in this project is expected to be incorporated in the new framework (see below).

While this project was focussed on agricultural lands, the majority of Albertans reside in urban areas. Rapid expansion of urban centers alters the hydrologic cycle in newly developed areas, in which groundwater recharge and discharge have a major influence on the hydrology of streams and wetlands. Therefore, it is beneficial to develop the knowledge further to evaluate

the effects of urbanization on groundwater recharge and discharge. This topic is a major focus of the new AI-WIP project (see 7.4.2 above). For this new project, we formed a partnership with the City of Calgary and the Town of Okotoks, in addition to AEP and other local watershed organizations.

9. KNOWLEDGE DISSEMINATION

In addition to scientific publications and conferences, the knowledge generated in the project was disseminated to the Government of Alberta through a technical report of AER/AGS (section 6.3.3) and participation of the investigators in the advisory panel for AEP's Groundwater Management Framework. The knowledge is also disseminated through presentations at the annual Water Innovation Forum of Alberta Innovates, as well as other public outreach venues including:

Hayashi, M. Hydrology of prairie wetlands: Scientific foundation for management and conservation. Seminar given to the staff of Matrix-Solutions Ltd., Guelph, Ontario, July 27, 2017.

Hayashi, M. Hydrology of prairie wetlands: Scientific foundation for management and conservation. Seminar given for the International Association of Hydrogeologists – Saskatchewan Local Chapter, Regina, Saskatchewan, May 4, 2018.

Hayashi, M. Reducing the uncertainty in groundwater availability and its sensitivity to land-use and climate variability. Seminar given for the Engineers Without Borders Calgary Chapter, Calgary, Alberta, January 14, 2019.

Hayashi, M. Effects of agricultural land-use practices on prairie hydrology and groundwater recharge. Online seminar given for Natural Resources Conservation Board of Alberta, November 9, 2020.

The new knowledge is incorporated in a graduate-level course on 'Surface water – groundwater interaction: From watershed processes to hyporheic exchange'. The course was attended by 12 employees from AEP and AF in July 2017 and five employees from AEP in Fall 2020. The research results are also incorporated in a graduate level course on 'Groundwater resources management', which is attended by those students who will become groundwater managers in Alberta and elsewhere.

10. CONCLUSIONS

Groundwater recharge is fundamental to the evaluation of sustainable water extraction rates from the aquifers in Alberta. The overall goal of this project was to advance our understanding of recharge processes in the unique environment of the Canadian prairies and develop practical tools for recharge estimation. The key project components were the following. (1) Evaluation of the spatial variability of recharge processes. (2) Comparison of groundwater recharge under grasslands and croplands. (3) Examination of groundwater recharge processes under irrigated fields. (4) Watershed-scale assessment of groundwater recharge. (5) Assessment of climate-change impacts on groundwater recharge.

Detailed field observation at instrumented study sites showed that depression-focussed recharge is the dominant mode of groundwater recharge in both grasslands and croplands, confirming the results of previous studies in Alberta and Saskatchewan. A simple numerical model was developed to simulate depression-focussed recharge. The model simulation results were consistent with field observations at a scale of individual depressions (10^2-10^3 m^2) and at a scale of a small watershed (10^2 km^2).

The land-use comparison study showed that snowmelt runoff generation in grazed grasslands was only moderately greater than in croplands under zero-tillage. This is contrary to previous studies that reported much greater runoff in croplands under conventional tillage than in ungrazed grasslands. Considering that snowmelt runoff is a major driver of depression-focussed groundwater recharge, the common agricultural land-use practices in Alberta, namely grazing and crop production, may not have a large influence on recharge processes. However, it is important to consider the combined effects of land use and topography, because grasslands are commonly associated with higher-relief terrain, which tend to generate a greater amount of runoff compared to lower-relief terrain used for crop production.

The key finding of the irrigation study is that groundwater recharge is focussed under depressions even when the fields are irrigated, even though a limited amount of recharge occurred under irrigated uplands. This is likely because the irrigation rates were optimized to minimize the deep percolation of irrigated water below the root zone of annual crops.

The numerical recharge model, VSMB-DUS was used to estimate the spatial distribution of groundwater recharge in the agricultural region (i.e. White Zone) of central and southern Alberta under the present climate. The results showed that the recharge amounts varied between 5 and 60 mm y^{-1}. The values were generally lower in the southeastern part of the region and higher in the northwestern part, reflecting the climatic gradient.

Using the dynamically downscaled climate model outputs representing hydrological years 2095-2100 under the 'business as usual' greenhouse gas emission scenario, groundwater recharge amounts were estimated for the agricultural region of central and southern Alberta. In general, groundwater recharge rates are expected to remain the same or slightly decline due to the reduction in snowmelt runoff. However, the climate model indicates increased amounts and intensity of rainfall during the growing season, generating high summer runoff in wet years. As a result, the timing of recharge may shift from spring to summer and the amounts may increase in wet years.

The primary benefit of this project is the spatially distributed information on groundwater recharge in the agricultural region of Alberta, and a simple numerical tool to estimate groundwater recharge at a local site using the basic soil and meteorological information. This type of information will be valuable for assessing the potential impacts of increased groundwater extraction at scales ranging from individual farmlands to watersheds. The secondary benefits of the project are the strengthened collaboration between the university researchers and Alberta Government departments, and the training of students and field technicians who have obtained meaningful employments using the skills learned through the project.

The next step of groundwater recharge studies is to understand the connection between the recharge of shallow water-table aquifers (or aquitards) and the induced recharge of deeper aquifers resulting from groundwater extraction, as well as the integrated understanding of

groundwater recharge and discharge at a scale of small watersheds. It is also important to understand the impacts of urbanization of previously rural watersheds in light of rapidly expanding urban centers in Alberta.

AKNOWLEGEMENT

We thank Stauffer family, Christensen family, and Perry family for making their farms available; Alberta Innovates, Alberta Environment and Parks, Alberta Energy Regulator / Alberta Geological Survey, and Alberta Agriculture and Forestry for providing cash and in-kind support and participating in the project steering committee; Lethbridge Demonstration Farm for land access and logistical support; Brandon Hill, Evan Sieben, and many student assistants for field work; and additional funding support from Natural Sciences and Engineering Research Council (CREATE for Water Security) and Global Water Futures (Prairie Water).

REFERENCES

Abdrakhimova, P. 2020. Improving groundwater flow model parameterization techniques. Ph.D. Thesis, University of Calgary.

Akinremi, O.O., S.M. McGinn and A.G. Barr. 1996. Simulation of soil moisture and other components of the hydrological cycle using a water budget approach. Canadian Journal of Soil Science 76: 133-142.

Baier, W. and G.W. Robertson. 1966. A new versatile soil moisture budget. Canadian Journal of Plant Science 46: 299-315.

Barker, A.A., Riddell, J.T.F., Slattery, S.R., Andriashek, L.D., Moktan, H., Wallace, S., Lyster, S., Jean, G., Huff, G.F., Stewart, S.A., and Lemay, T.G. 2011. Edmonton-Calgary Corridor groundwater atlas, Energy Resources Conservation Board, ERCB/AGS Information Series 140, 90 pp.

Cannon, A.J., 2018. Multivariate quantile mapping bias correction: an N-dimensional probability density function transform for climate model simulations of multiple variables. Climate Dynamics, 50, 31-49.

Dee, D.P., Uppala, S.M., Simmons, A.J., Berrisford, P., Poli, P., Kobayashi, S., Andrae, U., Balmaseda, M.A., Balsamo, G., Bauer, D.P. and Bechtold, P., 2011. The ERA‐Interim reanalysis: Configuration and performance of the data assimilation system. Quarterly Journal of the Royal Meteorological Society, 137, 553-597.

Diersch, H.-J.G. 2014. FEFLOW. Springer Berlin Heidelberg, Berlin, Heidelberg.

Fang, X. and Pomeroy, J.W. 2009. Modelling blowing snow redistribution to prairie wetlands. Hydrological Processes, 23, 2557-2569.

Fenton, M.M., Waters, E.J., Pawley, S.M., Atkinson, N., Utting, D.J., and Mckay, K. 2013. Alberta Geological Survey Map 601 Surficial Geology of Alberta.

Government of Alberta, 2020. Agricultural moisture situation update. Retrieved from http://agriculture.alberta.ca/acis/climate-maps.jsp [2020 May 18].

Hayashi, M., and Farrow, C.R. 2014. Watershed-scale response of groundwater recharge to inter-annual and inter-decadal variability in precipitation (Alberta, Canada). Hydrogeology Journal, 22, 1825-1839.

Hayashi, M., Jackson, J.F., and Xu, L. 2010. Application of the Versatile Soil Moisture Budget model to estimate evaporation from prairie grassland. Canadian Water Resources Journal, 35, 187-208.

Hayashi, M. and van der Kamp, G. 2000. Simple equations to represent the volume-area-depth relations of shallow wetlands in small topographic depressions. Journal of Hydrology, 237, 74-85.

Hayashi, M., van der Kamp, G., and Rudolph, D.L. 1998. Water and solute transfer between a prairie wetland and adjacent uplands, 2. Chloride cycle. Journal of Hydrology, 207, 56-67.

Healy, R.W., and Cook, P.G. 2002. Using groundwater levels to estimate recharge. Hydrogeology Journal, 10, 91-109.

Hughes, A. 2019. Investigating groundwater recharge rates and seasonality under irrigated and dryland conditions at two agricultural sites near Lethbridge, Alberta. MSc Thesis, University of Calgary.

Klassen, J., Liggett, J.E., Pavlovskii, I., and Abdrakhimova, P. 2018. First-order groundwater availability assessment for southern Alberta. Alberta Energy Regulator / Alberta Geological Survey. AER/AGS Open File Report 2018-09. 37pp.

Li, Y., Li, Z., Zhang, Z., Chen, L., Kurkute, S., Scaff, L., and Pan, X. 2019. High-resolution regional climate modeling and projection over western Canada using a weather research forecasting model with a pseudo-global warming approach. Hydrology and Earth System Sciences, 23, 4635-4659.

Little, K.E., Hayashi, M., and Liang, S. 2016. Community-based groundwater monitoring network using a citizen-science approach. Groundwater, 54, 317–324.

Maathuis, H. and van der Kamp, G. 2006. The Q20 concept: Sustainable well yield and sustainable aquifer yield. Saskatchewan Research Council Publication No. 10417-4E06.

MacCormack, K. E., Atkinson, N., and Lyster, S. 2015. Sediment thickness of Alberta. Alberta Energy Regulator, AER/AGS Map 603.

MacMillan, R. A. and Pettapiece, W.W. 2000. Alberta Landforms: Quantitative morphometric descriptions and classification of typical Alberta landforms. Technical Bulletin No. 2000-2E. Research Branch, Agriculture and Agri-Food Canada, Semiarid Prairie Agricultural Research Centre, Swift Current, SK. 118 pp.

Mekis, E., and Vincent, L.A. 2011. An overview of the second generation adjusted daily precipitation dataset for trend analysis in Canada. Atmosphere-Ocean, 49, 163-177.

Mohammed, G.A., Hayashi, M., Farrow, C.R., and Takano, Y. 2013. Improved characterization of frozen soil processes in the Versatile Soil Moisture Budget model. Canadian Journal of Soil Science, 93, 511-531.

Morgan, L.R. 2019. Land use effects on depression-focused groundwater recharge in the prairies. M.Sc. thesis, University of Calgary, 128 pp.

Natural Resources Conservation Service. 2004. National Engineering Handbook, Part 630 Hydrology, Chapters 4-10. United States Department of Agriculture.

Niazi, A., Bentley, L.R. and Hayashi, M. 2017. Estimation of spatial distribution of groundwater recharge from stream baseflow and groundwater chloride. Journal of Hydrology, 546, 380-392.

Noorduijn, S.L., Hayashi, M. and Mohammed, G.A. and Mohammed, A.A., 2018. A coupled soil water balance model for simulating depression-focused groundwater recharge. Vadose Zone Journal, 17, 170176, doi:10.2136/vzj2017.10.0176.

Parsons, D.F., Hayashi, M. and van der Kamp, G. 2004. Infiltration and solute transport under a seasonal wetland: Bromide tracer experiments in Saskatoon, Canada. Hydrological Processes, 18, 2011-2027.

Pavlovskii, I., Hayashi, M. and Cey, E.E. 2019. Estimation of depression-focussed groundwater recharge using chloride mass balance: problems and solutions across scales. Hydrogeology Journal, 27, 2263-2278.

Pavlovskii, I., Noorduijn, S.L., Liggett, J.E., Klassen, J., and Hayashi, M. 2020. Quantifying terrain controls on runoff retention and routing in the Northern Prairies. Hydrological Processes, 34, 473-484.

Rodvang, J. 2002. Groundwater at the Canada-Alberta Crop Development Initiative (CACDI) Demonstration Farm. Irrigation Branch, Alberta Agriculture, Food and Rural Development, Lethbridge, Alberta.

Scanlon, B.R., Keese, K.E., Flint, A.L., Flint, L.E., Gaye, C.B., Edmunds, W.M., and Simmers, I. 2006. Global synthesis of groundwater recharge in semiarid and arid regions. Hydrological Processes, 20, 3335-3370.

Shetsen, I. 1987. Quaternary geology, southern Alberta. Alberta Research Council, ARC/AGS Map 207.

Shetsen, I. 2005. Surficial geology of Lethbridge, Alberta, NTS 82H and NTS 82I. Alberta Energy Regulator, AER/AGS Map 206.

Skamarock, W. C., Klemp, J. B., Dudhia, J., Gill, D. O., Barker, D. M., Wang, W., and Powers, J. G., 2008. A description of the Advanced Research WRF version 3. NCAR Technical note-475+ STR.

Tarboton, D.G. and Luce, C.H. 1996. Utah energy balance snow accumulation and melt model (UEB). Utah Water Research Laboratory.

Teutschbein, C. and Seibert, J. 2012. Bias correction of regional climate model simulations for hydrological climate-change impact studies: Review and evaluation of different methods. Journal of hydrology, 456, 12-29.

van der Kamp, G., Hayashi, M., and Gallén, D. 2003. Comparing the hydrology of grassed and cultivated catchments in the semi-arid Canadian prairies. Hydrological Processes, 17, 559-575.

van Dijk, T. 2005. Depression-focused recharge and the impacts of land use on the hydrology of small depressions in Calgary, Alberta. MSc. Thesis, University of Calgary, 158 pp.

Vincent, L.A., Wang, X.L., Milewska, E.J., Wan, H., Yang, F., and Swail, V. 2012. A second generation of homogenized Canadian monthly surface air temperature for climate trend analysis. Journal of Geophysical Research – Atmosphere, 117, doi:10.1029/2012JD017859.